Arachidonate 12/15-lipoxygenase-induced inflammation and oxidative stress are involved in the development of Diabetic Cardiomyopathy

Hirofumi Suzuki[1,5], Yosuke Kayama[2,5], Masaya Sakamoto[1,5], Hiroyuki Iuchi[1] , Ippei Shimizu[3], Takuya Yoshino[2] , Daisuke Katoh[2] , Tomohisa Nagoshi[2] , Katsuyoshi Tojo[1], Tohru Minamino[3,4], Michihiro Yoshimura[2], Kazunori Utsunomiya[1]

[1] Division of Diabetes, Metabolism and Endocrinology, Department of Internal Medicine, Jikei University School of Medicine, 3-25-8 Nishi-Shinbashi, Minatoku, Tokyo 105-0003, Japan
[2] Division of Cardiology, Department of Internal Medicine, Jikei University School of Medicine, 3-25-8 Nishi-Shinbashi, Minato-ku, Tokyo 105-0003, Japan
[3] Department of Cardiovascular Biology and Medicine, Niigata University Graduate School of Medical and Dental Sciences, 2-746 Asahimachidori, Chuoku Niigata 951–8518, Japan
[4] PRESTO, Japan Science and Technology Agency, 4-1-8 Honcho Kawaguchi, Saitama 332-0012, Japan
[5] These authors contributed equally to this work.

Address correspondence to:
Yosuke Kayama, MD, PhD
Division of Cardiology, Department of Internal Medicine, Jikei University School of Medicine, Jikei University School of Medicine, 3-25-8 Nishi-Shinbashi, Minato-ku, Tokyo 105-8461, Japan
Tel: +81-3-3433-1111
Fax: +81-3-3459-6043
Email: kayama@jikei.ac.jp

Abstract

Diabetes mellitus affects cardiac structure and function, and it has been suggested that diabetes leads to cardiomyopathy. Arachidonate 12/15-lipoxygenase (12/15-LOX) has been suggested to play an important role in atherogenesis and heart failure. However, the role of 12/15-LOX in diabetic cardiomyopathy has not been examined. In this study, we investigated the effects of cardiac 12/15-LOX on diabetic cardiomyopathy. We created streptozotocin (STZ)-induced diabetic mice and compared to those of *Alox15 deficient* (12/15-LOX KO) mice. Expression of 12/15-LOX as well as TNF-α and NF-κB were up-regulated in STZ-induced diabetic hearts. Disruption of 12/15-LOX significantly improved STZ-induced cardiac dysfunction and fibrosis. Moreover deletion of 12/15-LOX inhibited the increases of TNF-α and NF-κB as well as the production of STZ-induced reactive oxygen species (ROS) in the heart. Administration of N-acetylcysteine (NAC) in diabetic mice prevented STZ-induced cardiac fibrosis. Neonatal cultured cardiomyocytes exposed to high glucose condition induced the expression of 12/15-LOX as well as TNF-α, NF-κB and collagen markers. These increases were inhibited by treatment of 12/15-LOX inhibitor. Our results suggest that cardiac 12/15-LOX-induced inflammation and oxidative stress are involved in the development of diabetic cardiomyopathy and that inhibition of 12/15-LOX could be a novel treatment for this condition.

Keywords:

Inflammation, Oxidative stress, diabetic cardiomyopathy, 12/15-lipoxygenase

Non-standard Abbreviations and Acronyms:

12/15-LOX	12/15-lipoxygenase
12/15-HETE	12/15-Hydroxyeicosatetraenoic acid
CDC	Cinnamyl-3,4-dihydroxy-α-cyanocinnamate
FS	fractional shortening
LVDs	left ventricular systolic dimension
STZ	Streptozotocin
4-HNE	4-Hydroxy-2-nonenal
ROS	Reactive oxygen species
NADPH	nicotinamide adenine dinucleotide phosphate
Nox2	nicotinamide adenine dinucleotide phosphate oxidase 2
Nox4	nicotinamide adenine dinucleotide phosphate

	oxidase 4
NAC	N-acetylcysteine
NF-κB	nuclear factor -kappa B
TNF-α	Tumor necrosis factor-alpha
collagen1α2	collagen type I alpha2
collagen3α1	collagen type lll alpha1
Bip	immunoglobulin-heavy-chain-binding protein
CHOP	C/EBP-binding protein homologous protein

Introduction

Recently, the incidence of diabetes mellitus has increased rapidly, due to worldwide changes in lifestyle. The epidemic of obesity together with sedentary lifestyles are projected to result in over 300 million people having diabetes by 2025(1). According to the Framingham study, the relative rate of onset of heart failure in the diabetes is significantly high, and onset of heart failure leads to a poor prognosis for diabetes patients(2). Diabetes is an independent risk factor for heart failure. In addition, the number of cases of heart failure combined with diabetes continues to rise, and treatment will become a significant problem in the future(3). However, the detailed molecular mechanism underlying development of this pathological condition has not been elucidated yet(4; 5).

Arachidonic acid (AA) is a free fatty acid that is released from the cell membrane in response to various cytokines, peptides, and growth factors that become active under inflammatory conditions(6). There are three families of enzymes involved in the oxidative metabolism of AA. These include the LOXs, which produce hydroxyeicosatetraenoic acids (HETEs), the cyclooxygenases (COX-1 and COX-2) and cytochrome P-450 monooxygenases (7). The human LOX enzymes include 5-LOX, 12-LOX and 15-LOX(8; 9). LOX enzymes are named according to the specific carbon atoms of arachidonic acid that are oxidized. Thus, 12/15-LOX is a member of the LOX family that catalyzes the step from arachidonic acid to 12(S)-HETE and 15(S)-HETE(10). 12/15-LOX was originally isolated from porcine leukocytes(11), but its tissue distribution is now known to be relatively wide, including blood vessels, the brain, and the kidney(12).

Several lines of evidence have suggested that 12/15-LOX may play an important role in the development of atherosclerosis, nephropathy and neuropathy in diabetes mellitus(13-16). However, there is currently little evidence about a role played by 12/15-LOX in the development of diabetic cardiomyopathy. Therefore, we focused on the role of 12/15-LOX as a key molecule related to diabetic cardiomyopathy.

In the present study, we found that 12/15-LOX expression was significantly up-regulated in the heart of diabetic mice. We have shown that diabetes-induced activation of cardiac 12/15-LOX increased inflammation and oxidative stress in the diabetic heart. Conversely, disruption of 12/15-LOX reduces inflammation, oxidative stress and fibrosis in the diabetic heart, thereby improving systolic dysfunction. These findings suggest that inhibition of 12/15-LOX could be a novel treatment for diabetic cardiomyopathy.

Research Design and Methods

Animal models. All experimental protocols were approved by Jikei University review board. Male C57BL/6 and *Alox15-deficient* (12/15-LOX KO) mice aged 7 weeks were used in this study. *Alox15-deficient* mice on a C57BL/6 background were purchased from The Jackson Laboratory. For the diabetic model, 7-week-old male C57BL/6 and *Alox15-deficient* mice were intraperitoneally injected with a single dose of streptozotosin (STZ) at 150mg/kg body weight (Wako 545-00283). One week after induction of diabetes, the antioxidant N-acetylcysteine (NAC) (SIGMA 9165) was administered to the three groups in the drinking water for 15 weeks (average 1.44 g/kg/day). 12/15-LOX inhibitor cinnamyl-3,4-dihydroxy-cyanocinnamate (CDC, BIOMOL International, LP)(17), 8mg/kg once a day, was administered by subcutaneous injection for 4 weeks after induction of diabetes. We purchased the male db/db mice aged 11 weeks from CLEA Japan, Inc and used in this study.

Physiological and histological analysis. Echocardiography was performed with a Vevo 770 High Resolution Imaging System (Visual Sonics Inc.). To minimize variability of the data, heart rate was ~500-600 beats per minute when cardiac function was assessed. Average systolic pressure and heart rate were recorded by a photoelectric pulse device (Softron BP-98A, Softron Co) placed on the tail of conscious mice. 4-μm frozen cross sections of the heart were fixed in 4% paraformaldehyde and subjected to immunofluorescence staining for 12/15-LOX (Abcam ab87353), 4-Hydroxy-2-nonenal (4-HNE) (abcam ab20953) and Wheat germ agglutinin. Nuclei were stained with Hoechst (Life technologies Japan H3570). Pictures were taken on a Biorevo microscope (Keyence, BZ-9000). Cardiac tissue was fixed by perfusion with 20% Formalin Neutral Buffer Solution (Wako 136-10041), sectioned at 4-μm thickness and stained. For measurement of the percent area of cardiac fibrosis (% cardiac fibrosis), we selected 5 fields at random and calculated the ratio of Masson-stained fibrosis area to total myocardium area with the software “Photoshop CS5” (Adobe Systems Inc.) as described previously(18).

RNA analysis. Total RNA was isolated from the hearts of mice with RNA-Bee Reagent (Cosmo Bio Inc.). In brief, after preparing total RNA, first-strand cDNA was synthesized with QuantiTect® Reverse Transcription (QIAGEN Inc.). Real-time PCR was performed using Thermal Cycler Dice TP800 (TAKARA Bio Inc.) with SYBR® Premix Ex Taq™ II (TAKARA Bio Inc.) according to the manufacturer’s instructions. The specific oligonucleotide primers for GAPDH, TNF-α, collagen1α2 and collagen3α1

were selected using Primer3 (v. 0.4.0) (http://frodo.wi.mit.edu/).

Western blot analysis. Whole cell lysates were prepared in RIPA buffer (Sigma-Aldrich Japan Ltd. R0278). Lysates (30 μg) were resolved by SDS-PAGE. Proteins were transferred to a PVDF membrane (Life Technologies Co. Ltd.), which was incubated with the primary antibody, followed by anti-mouse, anti-rabbit IgG, light chain specific (The Jackson Laboratory). Specific proteins were detected using enhanced chemiluminescence (ECL Prime) (GE Healthcare). The primary antibodies used for Western blotting were as follows: 4-HNE (abcam ab20953), α-Tubulin (Santa Cruze Biotechnology, Inc sc-5286) and actin (Sigma-Aldrich Japan Ltd. A4700), NF-κB p50, phosphor-NF-κB p65 (Cell Signaling Technologies #3035, #3039), Histone H3 (Cell Signaling Technologies #3638), Bip, CHOP (Cell Signaling Technologies #3183, #2895). ELISA was performed according to the manufacturer's instructions to examine the levels of 12(S)-HETE and 15(S)-HETE (Assay Designs). We used the NE-PER® (Nuclear and Cytoplasmic Extraction kit, Thermo Fisher Scientific Inc.) for the extraction of nuclear proteins. NIH ImageJ software was used (http://rsbweb.nih.gov/ij/) to analyze intensity of Western blot bands.

Cell culture. Cardiomyocytes and cardiac fibroblasts were prepared from neonatal rats and cultured as described previously(19). Cardiomyocytes and cardiac fibroblasts were exposed to a high glucose concentration (25 mmol/L glucose; HG) and harvested at the indicated time points. Those were treated with normal glucose concentration (5.5 mmol/L glucose; LG) and 19.5mM mannitol to control for osmolarity.
Cardiomyocytes were cultured in media with HG with or without 10μM CDC and 1mM N-acetyl-L-cysteine (NAC, Sigma-Aldrich Japan Ltd.) or with LG for 24-72 hours at 37°C. Palmitic acids (100uM) were treated after 48 hours after split of cardiomyocyte and incubated for 24 hours.

Measurement of intracellular ROS in cardiomyocytes. We assayed ROS production by using chloromethyl-2,7-dichlorodihydro-fluorescein diacetate (CM-H2DCFDA; Invitrogen C6827). Cardiomyocytes were cultured with 5μM CM-H2DCFDA at 37℃ in the dark for 30 min and fixed the formation. CDC (10μM) was added 30min before treatment of high glucose. Pictures were taken on a Biorevo microscope (Keyence, BZ-9000). Fluorescence intensity was assessed for image analysis of the histogram by the software "Photoshop CS5".

Assessment of the mitochondrial membrane potential. The mitochondrial membrane potential ($\Delta \Psi m$) was assessed using Mito Tracker red. Briefly, cardiomyocytes were loaded with 0.5μM MitoTracker® Orange CMTMRos (Invitrogen M7510) at 37℃ for 30 min, washed and fixed the formation. Fluorescence intensity was assessed by the "Photoshop CS5".

Statistical analysis. Data are shown as the mean s.e.m. Multiple group comparisons were performed by one-way ANOVA, followed by Bonferroni's test for comparison of means. Comparisons between two groups were made using the two-tailed unpaired Student's *t* test or two-way ANOVA. In all analyses, $P < 0.05$ was considered statistically significant.

Results

Expression of 12/15-LOX pathway is up-regulated in the diabetic heart.

To determine whether 12/15-LOX is a key molecule in the development of diabetic cardiomyopathy, we examined the mRNA level of 12/15-LOX in the diabetic heart using PT-PCR. We created STZ-induced diabetic mice (WT-STZ) and compared them with control (saline) mice (WT). Cardiac expression of 12/15-LOX was significantly up-regulated with a peak at 4 weeks after STZ treatment in WT-STZ **(Figure 1A)**. We next examined a production of 12(S)-HETE and 15(S)-HETE, a major metabolite of 12/15-LOX. Production of 12(S)-HETE and 15(S)-HETE were also significantly increased in the hearts of WT-STZ compared them with WT through the protocol until 16 weeks after STZ treatment **(Figure 1B)**. Immunohistochemistry showed that expression of 12/15-LOX was specifically up-regulated in cardiomyocytes of diabetic heart, but not in vascular cell and fibroblast cell **(Figure 1C)**.

Animal characteristics of Wild and Alox15-deficient mice after STZ treatment

To investigate the relationship between up-regulation of 12/15-LOX and STZ-induced diabetic cardiomyopathy, we created STZ-induced diabetic mice using *Alox15-deficient mice* (KO) and compared them to WT-STZ mice. Animals were divided into 4 groups (WT, KO, WT-STZ, KO-STZ). Blood pressure (systolic blood pressure; SBP, diastolic blood pressure; DPB), heart rate, plasma glucose levels and body weight, in each animal were measured at 0, 8 and 16 weeks after saline (WT, KO) or STZ (WT-STZ, KO-STZ) treatment. Single injection of STZ (150 mg/kg ip) to adult male mice resulted in strongly high plasma glucose levels for a week after STZ treatment. Same dose of saline was injected as a control. High dose STZ-induced model has been established as a diabetes model and recognized as a useful model of diabetic cardiomyopathy(13; 20). There was no difference in blood pressure and heart rate among the 4 groups under normal or STZ-induced high glucose conditions. Plasma glucose levels remained around 10mmol/L in WT and KO mice without STZ treatment. No difference in plasma glucose level was observed between WT and KO, WT-STZ and KO-STZ at every weeks of age. Although body weight was not a tendency to increase at advancing age in mice after STZ treatment than control mice, there was no difference between WT and KO, WT-STZ and KO-STZ **(Table)**.

Disruption of 12/15-LOX improves cardiac dysfunction and fibrosis induced by hyperglycemia.

Echocardiography was performed at 0, 8, 16 weeks after saline or STZ treatment and

compared between 4 groups. Fractional shortening (FS) was gradually impaired and left ventricular systolic dimension (LVDs) was increased in WT-STZ from 8 weeks after induction of diabetes compared with those of WT. In contrast, systolic dysfunction and left ventricular dilatation were not observed in KO and KO-STZ **(Figure 2A)**. Histological examination revealed that 16 weeks after induction of diabetes, the fibrotic area progressively extended to the peri-vascular and interstitial areas in WT-STZ heart compared to WT heart. This increase was significantly inhibited in KO-STZ heart compared to that of WT-STZ **(Figure 2B)**. Quantitative analysis revealed that % cardiac fibrosis was significantly decreased in KO-STZ compared to those of WT-STZ **(Figure 2C)**. These results suggest that 12/15-LOX affects cardiac dysfunction of STZ-induced diabetic cardiomyopathy and the increased expression of 12/15-LOX-induced by hyperglycemia might cause cardiac dysfunction and fibrosis.

Disruption of 12/15-LOX decreases cardiac inflammation and oxidative stress induced by hyperglycemia.

We next examined the expression of inflammatory cytokine genes by RT-PCR. We found that cardiac expression of tumor necrosis factor-α (TNF-α) was up-regulated in WT-STZ heart compared to WT heart **(Figure 3A)**. Cardiac collagen markers such as collagen1α2 and collagen3α1 were also increased in WT-STZ heart compared to WT heart at every four-week after STZ treatment, these increase were canceled by disruption of 12/15-LOX **(Figure 3B)**. Moreover, we examined the relationship between 12/15-LOX expression and activation of NF-κB in WT-STZ heart and KO-STZ heart by western blot analysis. Cardiac activation of NF-κB was up-regulated in WT-STZ heart compared to WT heart. This up-regulation of NF-κB was also inhibited by disruption of 12/15-LOX **(Figure 3C, 3D)**, indicating that 12/15-LOX may induce cardiac inflammation, which was involved in the development of STZ-induced diabetic cardiomyopathy.

12/15-LOX induces cardiac oxidative stress in the diabetic heart.

We examined the relationship between 12/15-LOX and cardiac oxidative stress in the diabetic heart. Immunohistological staining and western blotting showed that expression of cardiac 4-HNE, a major marker of oxidative stress, was up-regulated in myocardium in WT-STZ heart compared to WT heart, and this enhancement was significantly inhibited by disruption of 12/15-LOX **(Figure 4A, 4B, 4C)**. We next examined the nicotinamide adenine dinucleotide phosphate (NADPH) oxidase isoforms by RT-PCR at 4 weeks after induction of diabetes. Among the NADPH isoforms, expression of

nicotinamide adenine dinucleotide phosphate oxidase 4 (Nox4) but not nicotinamide adenine dinucleotide phosphate oxidase 2 (Nox2) was up-regulated in WT-STZ heart compared to WT heart and KO heart. This increase was also inhibited in KO-STZ heart **(Figure 4D)**.

To investigate the subcellular mechanism of the increase in reactive oxygen species (ROS) in the diabetic heart, intracellular ROS levels in cardiomyocytes were estimated under HG and LG by fluorimetry *in vitro*. Cardiomyocytes under HG showed enhancement of fluorescence intensity of DCF-DA by 7 fold at 24 hours compared to findings for those under LG (Figure 4E, 4F). Treatment with 12/15-LOX inhibitor (CDC) inhibited the enhancement of DCF-DA fluorescence under HG condition (Figure 4E, 4F). To further investigate the subcellular origins of ROS production in the diabetic heart, we used MitoTracker® Red to evaluate the effect of HG on the mitochondrial membrane potential in cardiomyocytes. The result showed that there was loss of mitochondrial membrane potential ($\Delta \Psi m$) as indicated by a decrease in the fluorescence intensity of MitoTracker® Red in cardiomyocytes under HG. This decrease in the fluorescence intensity was improved by treatment with CDC (Figure 4E, 4F).

These *in vivo* and *in vitro* results suggest that activation of NADPH oxidase and mitochondrial membrane abnormalities were occur in the diabetic heart and 12/15-LOX pathway is involved in the process of production of ROS and oxidative stress in the diabetic heart.

Cardiac fibrosis and inflammation are ameliorated by treatment with antioxidant in the diabetic heart

To investigate the relationship between cardiac oxidative stress and cardiac inflammation, we examined the hearts of WT-STZ mice who were administered the antioxidant N-acetylcysteine (NAC) in their drinking water (WT-STZ NAC) throughout the experimental period and compared them to the heart of WT, KO, WT-STZ and KO-STZ mice. NAC was administered to diabetic mice for 15 weeks and histological analysis and cardiac expressions of TNF-α, collagen1α2, and collagen3α1 were examined. Histological examination revealed that cardiac peri-vascular fibrosis was improved in WT-STZ NAC heart as well as KO-STZ heart compare to findings in the WT-STZ heart **(Figure 5A)**. Quantitative analysis revealed that the percentage of cardiac fibrosis was significantly decreased in KO-STZ and WT-STZ NAC hearts compared to those of WT-STZ hearts (**Figure 5B**). Moreover, RT-PCR showed that increased expression of TNF-α, collagen1α2 and collagen3α1 in WT-STZ NAC and KO-STZ hearts were significantly inhibited compare with the expressions in WT-STZ

hearts **(Figure 5C, 5D)**. These results indicate that cardiac oxidative stress has a major role in promoting cardiac inflammation in the STZ-induced diabetic heart.

Cardiac 12/15-LOX pathway induced by high glucose condition increases the expression of cardiac inflammation in vitro.

To further investigate the role of 12/15-LOX in cardiomyocytes under HG, we cultured neonatal cardiomyocytes under LG and HG using mannitol to adjust osmotic pressure for 24, 48 and 72 hours. RT-PCR showed that hyperglycemia up-regulated the expression of 12/15-LOX in cardiomyocytes **(Figure 6A)**. Production of 12(s)-HETE and 15(s)-HETE were also increased in cardiomyocytes under HG condition **(Figure 6B)**.

Furthermore, RT-PCR demonstrated the up-regulation of TNF-α, collagen1α2 and collagen3α1 in cardiomyocytes under HG after 24 hours **(Figure 6C, 6D)**. To determine whether increased expression of cardiac 12/15-LOX affects the up-regulation of TNF-α, collagen1α2 and collagen3α1 in cardiomyocyte, we cultured neonatal cardiomyocytes with CDC under HG and examined the expression of each markers. Increased expression of TNF-α, collagen1α2 and collagen3α1 under HG were inhibited by treatment with CDC **(Figure 6C, 6D)**. These results suggest that, cardiac 12/15-LOX induced by hyperglycemia implicated the up-regulation of inflammatory cytokines such as TNF-α, collagen1α2 and collagen3α1.

Treatment of antioxidant inhibits cardiac inflammation induced by high glucose condition in vitro

We next investigated the relationship between the oxidative stress and inflammation induced by hyperglycemia in cardiomyocytes. Treatment with NAC under HG, RT-PCR showed that up-regulation of TNF-α, collagen1α2 and collagen3α1 in cardiomyocytes was inhibited **(Figure 7A, 7B)**. Moreover, western blotting revealed that nucleus cardiac activation of NF-κB using anti-NF-κB p50 antibody and anti phospho-NF-κB p65 (Ser468) antibody was up-regulated under HG compared to under LG after 24 hours. This activation of NF-κB was significantly inhibited by treatment with NAC in cultured cardiomyocytes **(Figure 7C, 7D)**.

Discussion

In the present study we demonstrate that the arachidonate 12/15-LOX is an important molecule involved not only in the onset and development of diabetic cardiomyopathy, but also in increased inflammation and oxidative stress in the heart.

It has been known for a long time that after STZ administration, alternations occur in the enzymatic activity of cardiac contractile proteins, such as myosin and actomyosin, in rats and mice, and that cardiac contractile function gradually deteriorates(4; 21). This finding has provided a basis for the well-known diabetic cardiomyopathy model, where STZ administration quickly increases plasma glucose levels, and high plasma glucose levels are maintained for a long time, as shown in our experiments as well. In the hearts of wild-type mice exposed to increased plasma glucose levels, cardiac 12/15-LOX expression peaked at 4 weeks and its up-regulation persisted until 16 weeks after administration. Immunohistochemistry showed that the expression of 12/15-LOX in the heart was specifically up-regulated in cardiomyocytes but not in vascular and fibroblast cells. Cardiac function gradually deteriorated from 8 weeks onward after STZ administration, whereas this deterioration was suppressed in the *Alox15-deficient* mice. These results suggests that 12/15-LOX is involved in the onset and development of STZ-induced diabetic cardiomyopathy.

Arachidonic acid (AA) metabolites are known to be involved in the development of tissue inflammation and fibrosis in non-cardiovascular diseases such as pulmonary fibrosis (22; 23), suggesting an important role for AA as a potential pathway in the pathogenesis of cardiac fibrosis. A number of papers have demonstrated that the 12/15-LOX pathway induces inflammation in a variety of tissues. For example, overexpressed 12/15-LOX in macrophage-like J774.1 cells and HVSMC increased production of inflammatory cytokines such as interleukin-6 and TNF-α (24; 25). In an experimental asthma model, 12/15-LOX inhibition reduced airway inflammation and attenuated cell injury (26). Furthermore, 12/15-LOX caused cell growth of cardiac fibroblasts and matrix production in the heart (27) and mice with cardiac overexpression of 12/15-LOX showed increased the expressions of MCP-1 and TNF-α thereby inducing cardiac fibrosis and dysfunction (28). TNF-α is an important molecule that triggers inflammation and cell injury in the heart (29), which is known to induce cardiac fibrosis as

a consequence (30; 31). Its suppression has been shown to improve diabetic cardiomyopathy, reduce cardiac fibrosis, and recover cardiac function (21; 32; 33). In agreement with these findings, our results showed that the expressions of TNF-α and collagen markers were elevated accompanied by an increase in the expression of 12/15-LOX in the STZ-induced diabetic heart, whereas these increases were suppressed in the *Alox15-deficient* mice leading to cardiac function being preserved. Moreover, administration of a 12/15-LOX inhibitor (CDC) suppressed the up-regulation of TNF-α associated with high blood glucose levels *in vitro.* Our findings suggest that 12/15-LOX-induced TNF-α may have a major role in the development of cardiac fibrosis in STZ-induced diabetic cardiomyopathy.

Oxidative stress has been well-known to be involved in the development of diabetic cardiomyopathy, and increased ROS production is shown to induces various cardiovascular complications including cardiac dysfunction(32). Accumulating evidence suggests that mitochondria and NADPH oxidase are an important source of ROS production in the diabetic heart(34-36) where the crosstalk between mitochondria and NADPH oxidase are an important represents a feed-forward vicious cycle of ROS production(37; 38). It is important to elucidate the cellular mechanisms of ROS increase in the diabetic heart. Our histological examination revealed that cardiac production of 4-HNE was increased in the diabetic heart and DCF fluorescence showed that intracellular ROS levels in cardiomyocytes were increased under high glucose conditions. We also showed the cardiac expression of NOX4, one of the NADPH homologues, is elevated in the diabetic heart and the mitochondrial membrane potential is decreased in cardiomyocytes exposed to high glucose levels *in vitro*. Moreover, disruption of 12/15-LOX decreased the production of 4-HNE and expression of NOX4 in the diabetic heart, while a 12/15-LOX inhibitor (CDC) decreased intracellular ROS levels in cardiomyocytes and restored the mitochondrial membrane potential. These results suggest that oxidative stress is increased in the diabetic heart and that cardiomyocyte ROS production by mitochondria and NADPH oxidase plays a pivotal role in the onset and development of diabetic cardiomyopathy. Moreover, our results suggest that 12/15-LOX is an important molecule involved in the process of production of ROS and oxidative stress in the diabetic heart.

Recently, diabetic patients with hypertension have increased in

numbers with the risk of cardiovascular disease thought to be increased in these patients. Research into molecules involved in both diseases is of critical importance, given that any such molecule will likely represent a viable therapeutic target in the future. Diabetes not only causes hyperglycemia and increases oxidative stress, but also exhibits a complicated disease condition associated with concomitant hypertension eventually leading to atherosclerosis and organ injury(39). Persistent hyperglycemia associated with diabetes, insulin resistance, and postprandial hyperglycemia induces inflammation and oxidative stress and causes myocardial injury(40; 41). We previously confirmed by microarray analysis that 12/15-LOX was up-regulated in the heart of a hypertensive heart failure model and demonstrated that it is involved in the inflammation of the heart and development of cardiac fibrosis(28). Our present *in vivo* and *in vitro* studies demonstrate that 12/15-LOX is involved in the development of disease not only in the hypertensive heart failure model but also in the STZ-induced diabetic cardiomyopathy model, suggesting that 12/15-LOX is an important molecule affecting the heart in both diseases.

It has been shown that 12/15-LOX is involved in the onset of a variety of diseases associated with type 1 and type 2 diabetes, such as cardiovascular disease, hypertension, renal disease, and neurodegenerative disorders. Furthermore, the role of 12/15-LOX has been suggested in humans as well. Indeed, the expression of 12/15-LOX was shown to be an independent risk factor for atherosclerosis in 828 patients with diabetes(42), and 12/15-LOX inhibition is shown to lead to reductions in the size of cerebral infarction in humans(43-46).

We acknowledge several limitations of our study. First, not all groups were evaluated over the entire course of cardiac fibrosis development in the study. Second, we could not entirely exclude the effects of the pharmacological agents used, such as CDC and NAC, especially on cardiac fibrosis, due to lack of several control groups in the study. Furthermore, while we demonstrated that the active involvement of ROS in high glucose leads to the upregulation of 12/15-LOX, which, in turn, results in cardiac fibrosis, the precise mechanisms linking 12/15-LOX to profibrotic signaling still remain largely unknown. Despite these limitations, however, we believe we have provided important new insights into diabetic cardiomyopathy.

In conclusion, this study demonstrated the mechanisms through

which the expression of 12/15-LOX in the heart, associated with persistent hyperglycemia, leads to the development of diabetic cardiomyopathy via cardiac inflammation and oxidative stress. Moreover, it was suggested that inhibition of 12/15-LOX could potentially be a useful treatment for not only diabetic cardiomyopathy but also for diabetic complications.

Acknowledgments

No other potential conflicts of interest relevant to this article were reported. H.S. conducted experiments, performed data analyses and wrote the manuscript. Y.K. and M.S. designed research, analyzed data, and wrote the manuscript. I.S., H.I., T.Y.and K.T. contributed to experimental work (Staining analysis and animal care). T.N., K.T. and M.Y. contributed to discussion. T.M. designed research, analyzed data and contributed to reviewed/edited the manuscript. K.U. is the guarantor of this work and, as such, had full access to all the data in the study and takes responsibility for the integrity of the data and the accuracy of the data analysis. We thank Y. Inada and Y. Takada for research assistance and technical support (Division of Diabetes, Metabolism and Endocrinology, Department of Internal Medicine, Jikei University School of Medicine).

Sources of Funding

This work was supported by a Grant-in-Aid for Scientific Research from the Ministry of Education, Culture, Sports, Science and Technology of Japan, and from Uehara Memorial Foundation (to YK).

Author Information

The authors declare no competing financial interests.

Disclosures

None

Table ***Animal characteristics of Wild and Alox15-deficient mice after STZ treatment***

Wild type mice (WT) and *Alox15-deficient mice* (KO) were used to create a streptozotocin (STZ) –induced diabetic mce. Animals were divided into 4 groups (WT, KO, WT-STZ, KO-STZ). Blood pressure (Systolic blood pressure; SBP, Diastolic blood pressure ; DPB), heart rate, plasma glucose levels and body weight, in each animal were measured at 0, 8 and 16 weeks after saline (WT, KO) or STZ (WT-STZ, KO-STZ) treatment (Table 2). *P<0.05 vs. WT (0w), **P<0.01 vs. WT (0w), #P<0.05 vs. KO (0w), ##P<0.01 vs. KO (0w), † P<0.05 vs. WT (16w), ¶ P<0.05 vs. KO (16w). Results represent mean s.e.m. n=10-15.

	Wild (WT)				*Alox15-deficient* (KO)			
Parameters		0w	8w	16w		0w	8w	16w
Blood pressure (mmHg)								
(SBP)	WT	105.7(3.4)	100.2(2.1)	116.3(4.8)	KO	105.1(4.7)	100.8(4.7)	112.3(3.8)
	WT-STZ	108.1(5.0)	108.6(4.9)	120.7(3.9)	KO-STZ	105.7(4.7)	102.6(5.4)	117.7(2.6)
(DBP)	WT	58.2(3.1)	70.3(0.8)	63.7(4.1)	KO	62.1(3.2)	59.9(3.2)	68.7(4.4)
	WT-STZ	60.2(4.0)	65.9(3.7)	65.7(3.9)	KO-STZ	58.1(3.8)	57.5(4.4)	64.4(2.3)
Heart rate (bpm)	WT	627(19)	655(9)	665(22)	KO	631(19)	618(38)	646(14)
	WT-STZ	615(25)	583(35)	601(22)	KO-STZ	595(28)	593(32)	590(16)
Plasma glucose (mol/l)	WT	10.1(0.4)	11.9(1.0)	10.3(0.7)	KO	10.7(0.6)	11.8(0.7)	11.0(0.7)
	WT-STZ	10.3(0.6)	31.2(0.5)**	33.3(0.2)**	KO-STZ	10.1(1.1)	31.1(1.7)##	30.9(0.6)##
Body weight (g)	WT	22.6(0.4)	26.8(1.0)*	29.9(1.4)**	KO	19.6(0.8)	21.2(1.9)	26.1(0.9)#
	WT-STZ	22.4(1.0)	20.9(0.5)* †	23.4(1.0)*	KO-STZ	22.4(0.8)	20.8(0.6)	22.5(1.3)#,¶

Figure Legends

Figure 1 ***Expression of 12/15-LOX pathway is up-regulated in the diabetic heart.***

(A) Expression of 12/15-LOX in the hearts of wild-type (WT), wild-STZ (WT-STZ) mice by RT-PCR. Cardiac expression of 12/15-LOX was up-regulated in WT-STZ compared to WT at every weeks of age. (B) 12/15(S)-HETE levels in the hearts of WT and WT-STZ by ELISA. Production of 12/15(S)-HETE was increased in the hearts of WT-STZ compared to WT. *P<0.05 **P<0.01 WT-STZ vs. WT. Error bars indicate s.e.m. n= 10-15 in each group. (C) Immunofluorescence staining of 12/15-LOX in the hearts of WT and WT-STZ at 4 weeks after induction of diabetes. Expression of 12/15-LOX (red) was specifically up-regulated in cardiomyocytes of diabetic hearts. Wheat germ agglutinin (WGA) was used to label cardiomyocytes membranes (green). Upper panel is the staining of cardiomyocytes membranes (green). Middle panel is the staining of 12/15-LOX (red). Lower panel is the merged image of 12/15-LOX, cardiomyocytes membranes and hoechst staining. Scale bar, 60μm.

Figure 2 ***Disruption of 12/15-LOX improves cardiac dysfunction and fibrosis induced by hyperglycemia.***

(A) Echocardiographic findings in wild-type (WT), wild-STZ (WT-STZ), *Alox15-deficient* (KO) and *Alox15-deficient*-STZ (KO-STZ) mice. Left ventricular FS was gradually decreased and the LVDd was increased in WT-STZ compared with WT. These changes observed in WT-STZ were further exacerbated by aging. FS and LVDs were improved in KO-STZ compared to WT-STZ. *P<0.05 vs. WT, $^{\#}$P<0.05 vs. KO-STZ (16w). Error bars indicate s.e.m. n= 10-15 in each group

(B) Masson Trichrome staining in the hearts of WT, WT-STZ, KO-STZ at 16 weeks after induction of diabetes. An increase in peri-vascular and interstitial fibrosis was observed in WT-STZ; this fibrosis decreased in KO-STZ mice. Scale bar, 60μm. The percentage area of fibrosis in the hearts of WT, WT-STZ and KO-STZ. *P<0.05 vs. WT, $^{\#}$P<0.05 vs WT-STZ. Error bars indicate s.e.m. n=7-10.

Figure 3 ***Disruption of 12/15-LOX decreases cardiac inflammation and oxidative stress induced by hyperglycemia.***

(A, B) RT-PCR analysis for tumor necrosis factor-α (TNF-α), collagen markers collagen1α2 and collagen3α1 in the hearts of wild-type (WT), wild-STZ (WT-STZ) and *Alox15-deficient*-STZ (KO-STZ) mice at 4-16 weeks after induction of diabetes. Cardiac expression of TNF-α, collagen1α2 and collagen3α1 was up-regulated in

WT-STZ compared to WT hearts. These increases were also inhibited by disruption of 12/15-LOX. *P<0.05 **P<0.01 vs. WT, #P<0.05 ##P<0.01 vs. WT-STZ. Error bars indicate s.e.m. n=7-10. (C) Western blot analysis of NF-κB activation in the hearts of WT, WT-STZ and KO-STZ using anti-histone antibody and anti-NF-κB p50 antibody. We extracted the nuclear proteins of NF-κB p50 by using Nuclear and Cytoplasmic Extraction kit. (D) Analyzing intensity of Western blot bands showed that cardiac activation of NF-κB was up-regulated in WT-STZ heart compared to WT heart. The increased expression of NF-κB was also inhibited by disruption of 12/15-LOX. *P<0.05 vs. WT, #P<0.05 vs. WT-STZ. Data are shown as mean+s.e.m of duplicates and are representative of 1 experiment out of 5.

Figure 4 ***12/15-LOX induces the cardiac oxidative stress in the diabetic heart.***
(A) Immunohistological staining (brown) of 4-Hydroxy-2-nonenal (4-HNE) in the hearts of wild-type (WT), *Alox15-deficient* (KO), wild-STZ (WT-STZ) and *Alox15-deficient*-STZ (KO-STZ) mice. Upper panel is x20, lower panel is x400, Scale bar, 1mm and 30μm. (B) Western blot analysis of 4-HNE expression in the hearts of WT, KO, WT-STZ and KO-STZ using anti-4-HNE antibody and anti-actin antibody. (C) Analyzing intensity of Western blot bands showed that cardiac 4-HNE level (38kD) was significantly increased in WT-STZ compared to WT hearts and this increase was significantly inhibited by disruption of 12/15-LOX. *P<0.05 vs. WT, #P<0.05 vs. KO-STZ. Data are shown as mean+s.e.m of duplicates and are representative of 1 experiment out of 5. (D) RT-PCR analysis for NADPH oxidase 2 (Nox2) and 4 (Nox4) in the hearts of WT, KO, WT-STZ and KO-STZ was examined at 4 weeks after induction of diabetes. *P<0.05 vs. WT, #P<0.05 vs. WT-STZ. Error bars indicate s.e.m. n=4-6. (E) Representative images of CM-H2DCFDA and MitoTracker® Orange CMTMRos fluorescence in cultured neonatal cardiomyocytes under normal glucose (LG), high glucose (HG) and high glucose+12/15-LOX inhibitor (CDC 10μmol/L) (HG+CDC) groups. (F) Quantitative results of analysis. Treatment of CDC significantly attenuated the increase of ROS caused by high glucose condition. *P<0.05 vs. LG, #P<0.05 vs. HG. Error bars indicate s.e.m. n=4-6.

Figure 5 ***Cardiac fibrosis and inflammation are ameliorated by treatment with antioxidant in the diabetic heart.***
(A) Masson Trichrome staining in the hearts of wild-type (WT), *Alox15-deficient* (KO), wild-STZ (WT-STZ), *Alox15-deficient*-STZ (KO-STZ) and wild-STZ with NAC (WT-STZ+NAC) at 16 weeks after induction of diabetes. An increase in peri-vascular

and interstitial fibrosis was observed in WT-STZ; this fibrosis decreased in WT-STZ+NAC. Scale bar, 60μm. (B) The percentage area of fibrosis in the hearts of WT, KO, WT-STZ and WT-STZ+NAC. *P<0.05 vs. WT, $^{\#}$P<0.05 vs WT-STZ+NAC. Error bars indicate s.e.m. n=7-10. (C, D) RT-PCR analysis for TNF-α, collagen1α2 and collagen3α1 in the hearts of WT, KO, WT-STZ and WT-STZ+NAC at 4-16 weeks after induction of diabetes. Cardiac expression of TNF-α, collagen1α2 and collagen3α1 were up-regulated in WT-STZ compared with WT hearts. These increases were also inhibited by NAC. *P<0.05 **P<0.01 vs. WT, $^{\#}$P<0.05 $^{\#\#}$P<0.01 vs. WT-STZ+NAC. Error bars indicate s.e.m. n=5-10.

Figure 6 ***Cardiac 12/15-LOX pathway induced by hyperglycemia increases the expression of cardiac inflammation in vitro.***

Cardiomyocytes were treated with high glucose condition (25 mmol/L; HG) or normal glucose condition (5.5 mmol/L; LG) for the indicated times (0-72h). (A) Expression of 12/15-LOX in cardiomyocytes by RT-PCR. (B) Production of 12/15(s)-HETE in cardiomyocytes by ELISA. *P<0.05 vs. LG, $^{\#}$P<0.05 vs. HG. Error bars indicate s.e.m. n=4-7.

Cardiomyocytes were treated with 12/15-LOX inhibitor (CDC 10μmol/L) for the indicated time (24-72 hours). (C, D) Expression of TNF-α, collagen1α2 and collagen3α1 in cardiomyocytes treated with LG, HG and HG with CDC by RT-PCR.

Up-regulation of TNF-α, collagen1α2 and collagen3α1 under HG were inhibited by treatment with CDC. *P<0.05 vs. LG, $^{\#}$P<0.05 vs. HG. Error bars indicate s.e.m. n=4-7.

Figure 7 ***Treatment of antioxidant inhibit cardiac inflammation induced by high glucose condition in vitro.***

Cardiomyocytes were treated with high glucose condition (25 mmol/L; HG) or normal glucose condition (5.5 mmol/L; LG) for the indicated times (0-72h) (A, B) Expression of TNF-α, collagen1α2 and collagen3α1 in cardiomyocyte by RT-PCR. Up-regulation of TNF-α, collagen1α2 and collagen3α1 in cardiomyocytes under HG were inhibited by treatment with NAC. *P<0.05 vs. LG, $^{\#}$P<0.05 vs. HG. Error bars indicate s.e.m. n=4-7. (C) Western blot analysis of NF-κB activation in cardiomyocytes using anti-NF-κB p50 antibody, anti-phospho-NF-κB p65 (Ser468) antibody and anti-histone antibody. (D) Analyzing intensity of Western blotting showed that cardiac activation of NF-κB was up-regulated in HG compared to LG after 24 hours. The activation of NF-κB was also inhibited by treatment with NAC. *P<0.05 vs. LG, $^{\#}$P<0.05 vs. HG. Data are shown as mean+s.e.m of duplicates and are representative of 1 experiment out of 5.

References

1. King H, Aubert RE, Herman WH: Global burden of diabetes, 1995-2025: prevalence, numerical estimates, and projections. Diabetes care 1998;21:1414-1431

2. Currie CJ, Peters JR, Tynan A, Evans M, Heine RJ, Bracco OL, Zagar T, Poole CD: Survival as a function of HbA(1c) in people with type 2 diabetes: a retrospective cohort study. Lancet 2010;375:481-489

3. Boudina S, Abel ED: Diabetic cardiomyopathy revisited. Circulation 2007;115:3213-3223

4. Poornima IG, Parikh P, Shannon RP: Diabetic cardiomyopathy: the search for a unifying hypothesis. Circulation research 2006;98:596-605

5. Chavali V, Tyagi SC, Mishra PK: Predictors and prevention of diabetic cardiomyopathy. Diabetes, metabolic syndrome and obesity : targets and therapy 2013;6:151-160

6. Liscovitch M: Crosstalk among multiple signal-activated phospholipases. Trends in biochemical sciences 1992;17:393-399

7. Natarajan R, Nadler JL: Lipid inflammatory mediators in diabetic vascular disease. Arteriosclerosis, thrombosis, and vascular biology 2004;24:1542-1548

8. Chen XS, Funk CD: Structure-function properties of human platelet 12-lipoxygenase: chimeric enzyme and in vitro mutagenesis studies. FASEB journal : official publication of the Federation of American Societies for Experimental Biology 1993;7:694-701

9. Kuhn H, Walther M, Kuban RJ: Mammalian arachidonate 15-lipoxygenases structure, function, and biological implications. Prostaglandins & other lipid mediators 2002;68-69:263-290

10. Chen XS, Kurre U, Jenkins NA, Copeland NG, Funk CD: cDNA cloning, expression, mutagenesis of C-terminal isoleucine, genomic structure, and chromosomal localizations of murine 12-lipoxygenases. The Journal of biological chemistry 1994;269:13979-13987

11. Yokoyama C, Shinjo F, Yoshimoto T, Yamamoto S, Oates JA, Brash AR: Arachidonate 12-lipoxygenase purified from porcine leukocytes by immunoaffinity chromatography and its reactivity with hydroperoxyeicosatetraenoic acids. The Journal of biological chemistry 1986;261:16714-16721

12. Kuhn H, O'Donnell VB: Inflammation and immune regulation by 12/15-lipoxygenases. Progress in lipid research 2006;45:334-356

13. Shen E, Li Y, Li Y, Shan L, Zhu H, Feng Q, Arnold JM, Peng T: Rac1 is required for cardiomyocyte apoptosis during hyperglycemia. Diabetes 2009;58:2386-2395

14. Chinetti-Gbaguidi G, Baron M, Bouhlel MA, Vanhoutte J, Copin C, Sebti Y, Derudas B, Mayi T, Bories G, Tailleux A, Haulon S, Zawadzki C, Jude B, Staels B: Human atherosclerotic plaque alternative macrophages display low cholesterol handling but high phagocytosis because of distinct activities of the PPARgamma and LXRalpha pathways.

Circulation research 2011;108:985-995
15. Kang SW: Role of 12-Lipoxygenase in the Stimulation of p38 Mitogen-Activated Protein Kinase and Collagen 5(IV) in Experimental Diabetic Nephropathy and in Glucose-Stimulated Podocytes. Journal of the American Society of Nephrology 2003;14:3178-3187
16. Stavniichuk R, Shevalye H, Hirooka H, Nadler JL, Obrosova IG: Interplay of sorbitol pathway of glucose metabolism, 12/15-lipoxygenase, and mitogen-activated protein kinases in the pathogenesis of diabetic peripheral neuropathy. Biochemical pharmacology 2012;83:932-940
17. Pergola C, Jazzar B, Rossi A, Buehring U, Luderer S, Dehm F, Northoff H, Sautebin L, Werz O: Cinnamyl-3,4-dihydroxy-alpha-cyanocinnamate is a potent inhibitor of 5-lipoxygenase. The Journal of pharmacology and experimental therapeutics 2011;338:205-213
18. He X, Gao X, Peng L, Wang S, Zhu Y, Ma H, Lin J, Duan DD: Atrial fibrillation induces myocardial fibrosis through angiotensin II type 1 receptor-specific Arkadia-mediated downregulation of Smad7. Circulation research 2011;108:164-175
19. Sano M, Minamino T, Toko H, Miyauchi H, Orimo M, Qin Y, Akazawa H, Tateno K, Kayama Y, Harada M, Shimizu I, Asahara T, Hamada H, Tomita S, Molkentin JD, Zou Y, Komuro I: p53-induced inhibition of Hif-1 causes cardiac dysfunction during pressure overload. Nature 2007;446:444-448
20. Jin HR, Kim WJ, Song JS, Choi MJ, Piao S, Shin SH, Tumurbaatar M, Tuvshintur B, Nam MS, Ryu JK, Suh JK: Functional and morphologic characterizations of the diabetic mouse corpus cavernosum: comparison of a multiple low-dose and a single high-dose streptozotocin protocols. The journal of sexual medicine 2009;6:3289-3304
21. Westermann D, Walther T, Savvatis K, Escher F, Sobirey M, Riad A, Bader M, Schultheiss HP, Tschope C: Gene deletion of the kinin receptor B1 attenuates cardiac inflammation and fibrosis during the development of experimental diabetic cardiomyopathy. Diabetes 2009;58:1373-1381
22. Charbeneau RP, Peters-Golden M: Eicosanoids: mediators and therapeutic targets in fibrotic lung disease. Clinical science (London, England : 1979) 2005;108:479-491
23. Levick SP, Loch DC, Taylor SM, Janicki JS: Arachidonic acid metabolism as a potential mediator of cardiac fibrosis associated with inflammation. Journal of immunology (Baltimore, Md : 1950) 2007;178:641-646
24. Wen Y, Gu J, Chakrabarti SK, Aylor K, Marshall J, Takahashi Y, Yoshimoto T, Nadler JL: The role of 12/15-lipoxygenase in the expression of interleukin-6 and tumor necrosis factor-alpha in macrophages. Endocrinology 2007;148:1313-1322

25. Dwarakanath RS, Sahar S, Lanting L, Wang N, Stemerman MB, Natarajan R, Reddy MA: Viral vector-mediated 12/15-lipoxygenase overexpression in vascular smooth muscle cells enhances inflammatory gene expression and migration. Journal of vascular research 2008;45:132-142
26. Mabalirajan U, Ahmad T, Rehman R, Leishangthem GD, Dinda AK, Agrawal A, Ghosh B, Sharma SK: Baicalein reduces airway injury in allergen and IL-13 induced airway inflammation. PloS one 2013;8:e62916
27. Wen Y, Gu J, Liu Y, Wang PH, Sun Y, Nadler JL: Overexpression of 12-Lipoxygenase Causes Cardiac Fibroblast Cell Growth. Circulation research 2001;88:70-76
28. Kayama Y, Minamino T, Toko H, Sakamoto M, Shimizu I, Takahashi H, Okada S, Tateno K, Moriya J, Yokoyama M, Nojima A, Yoshimura M, Egashira K, Aburatani H, Komuro I: Cardiac 12/15 lipoxygenase-induced inflammation is involved in heart failure. The Journal of experimental medicine 2009;206:1565-1574
29. Nakamura K, Fushimi K, Kouchi H, Mihara K, Miyazaki M, Ohe T, Namba M: Inhibitory effects of antioxidants on neonatal rat cardiac myocyte hypertrophy induced by tumor necrosis factor-alpha and angiotensin II. Circulation 1998;98:794-799
30. Nelson DP, Setser E, Hall DG, Schwartz SM, Hewitt T, Klevitsky R, Osinska H, Bellgrau D, Duke RC, Robbins J: Proinflammatory consequences of transgenic fas ligand expression in the heart. The Journal of clinical investigation 2000;105:1199-1208
31. Duerrschmid C, Crawford JR, Reineke E, Taffet GE, Trial J, Entman ML, Haudek SB: TNF receptor 1 signaling is critically involved in mediating angiotensin-II-induced cardiac fibrosis. Journal of molecular and cellular cardiology 2013;57:59-67
32. Rajesh M, Mukhopadhyay P, Batkai S, Patel V, Saito K, Matsumoto S, Kashiwaya Y, Horvath B, Mukhopadhyay B, Becker L, Hasko G, Liaudet L, Wink DA, Veves A, Mechoulam R, Pacher P: Cannabidiol attenuates cardiac dysfunction, oxidative stress, fibrosis, and inflammatory and cell death signaling pathways in diabetic cardiomyopathy. Journal of the American College of Cardiology 2010;56:2115-2125
33. Westermann D, Van Linthout S, Dhayat S, Dhayat N, Schmidt A, Noutsias M, Song XY, Spillmann F, Riad A, Schultheiss HP, Tschope C: Tumor necrosis factor-alpha antagonism protects from myocardial inflammation and fibrosis in experimental diabetic cardiomyopathy. Basic research in cardiology 2007;102:500-507
34. Teshima Y, Takahashi N, Nishio S, Saito S, Kondo H, Fukui A, Aoki K, Yufu K, Nakagawa M, Saikawa T: Production of reactive oxygen species in the diabetic heart. Roles of mitochondria and NADPH oxidase. Circulation journal : official journal of the Japanese Circulation Society 2014;78:300-306
35. Bugger H, Boudina S, Hu XX, Tuinei J, Zaha VG, Theobald HA, Yun UJ, McQueen AP,

Wayment B, Litwin SE, Abel ED: Type 1 diabetic akita mouse hearts are insulin sensitive but manifest structurally abnormal mitochondria that remain coupled despite increased uncoupling protein 3. Diabetes 2008;57:2924-2932
36. Gorin Y, Block K: Nox as a target for diabetic complications. Clinical science (London, England : 1979) 2013;125:361-382
37. Dikalov S: Cross talk between mitochondria and NADPH oxidases. Free radical biology & medicine 2011;51:1289-1301
38. Lee SB, Bae IH, Bae YS, Um HD: Link between mitochondria and NADPH oxidase 1 isozyme for the sustained production of reactive oxygen species and cell death. The Journal of biological chemistry 2006;281:36228-36235
39. Node K, Inoue T: Postprandial hyperglycemia as an etiological factor in vascular failure. Cardiovascular diabetology 2009;8:23
40. Frustaci A, Kajstura J, Chimenti C, Jakoniuk I, Leri A, Maseri A, Nadal-Ginard B, Anversa P: Myocardial cell death in human diabetes. Circulation research 2000;87:1123-1132
41. Peterson LR, Herrero P, Schechtman KB, Racette SB, Waggoner AD, Kisrieva-Ware Z, Dence C, Klein S, Marsala J, Meyer T, Gropler RJ: Effect of obesity and insulin resistance on myocardial substrate metabolism and efficiency in young women. Circulation 2004;109:2191-2196
42. Burdon KP, Rudock ME, Lehtinen AB, Langefeld CD, Bowden DW, Register TC, Liu Y, Freedman BI, Carr JJ, Hedrick CC, Rich SS: Human lipoxygenase pathway gene variation and association with markers of subclinical atherosclerosis in the diabetes heart study. Mediators of inflammation 2010;2010:170153
43. van Leyen K, Kim HY, Lee SR, Jin G, Arai K, Lo EH: Baicalein and 12/15-lipoxygenase in the ischemic brain. Stroke; a journal of cerebral circulation 2006;37:3014-3018
44. Lebeau A, Terro F, Rostene W, Pelaprat D: Blockade of 12-lipoxygenase expression protects cortical neurons from apoptosis induced by beta-amyloid peptide. Cell death and differentiation 2004;11:875-884
45. Jin G, Arai K, Murata Y, Wang S, Stins MF, Lo EH, van Leyen K: Protecting against cerebrovascular injury: contributions of 12/15-lipoxygenase to edema formation after transient focal ischemia. Stroke; a journal of cerebral circulation 2008;39:2538-2543
46. Yigitkanli K, Pekcec A, Karatas H, Pallast S, Mandeville E, Joshi N, Smirnova N, Gazaryan I, Ratan RR, Witztum JL, Montaner J, Holman TR, Lo EH, van Leyen K: Inhibition of 12/15-lipoxygenase as therapeutic strategy to treat stroke. Annals of neurology 2012;

Figure1A

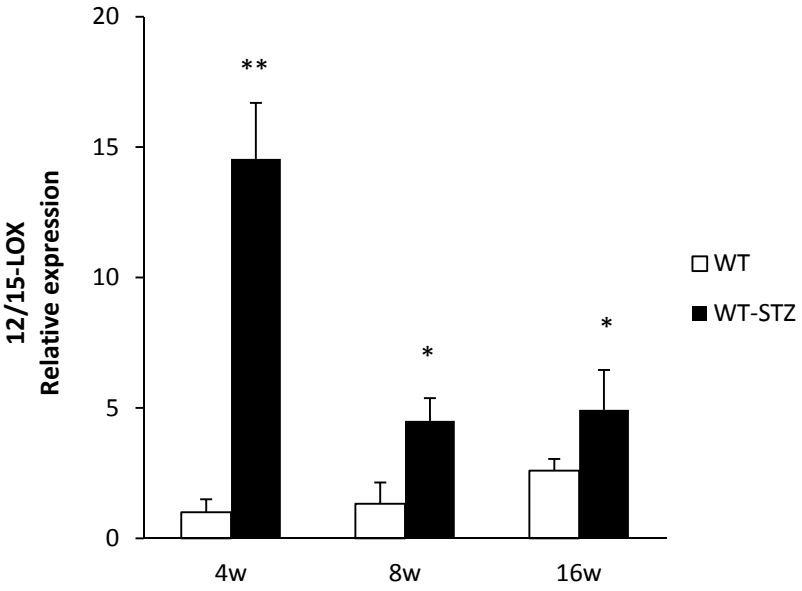

Figure1B

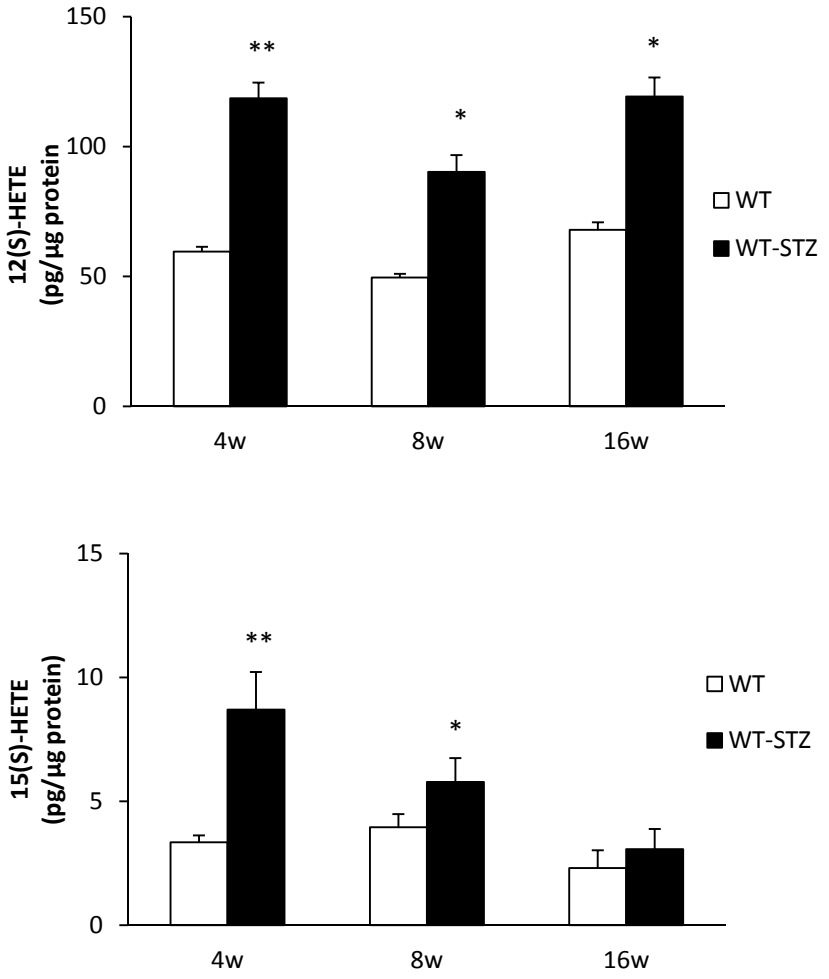

N=10-15, * : P<0.05, ** : P<0.01

Figure1C

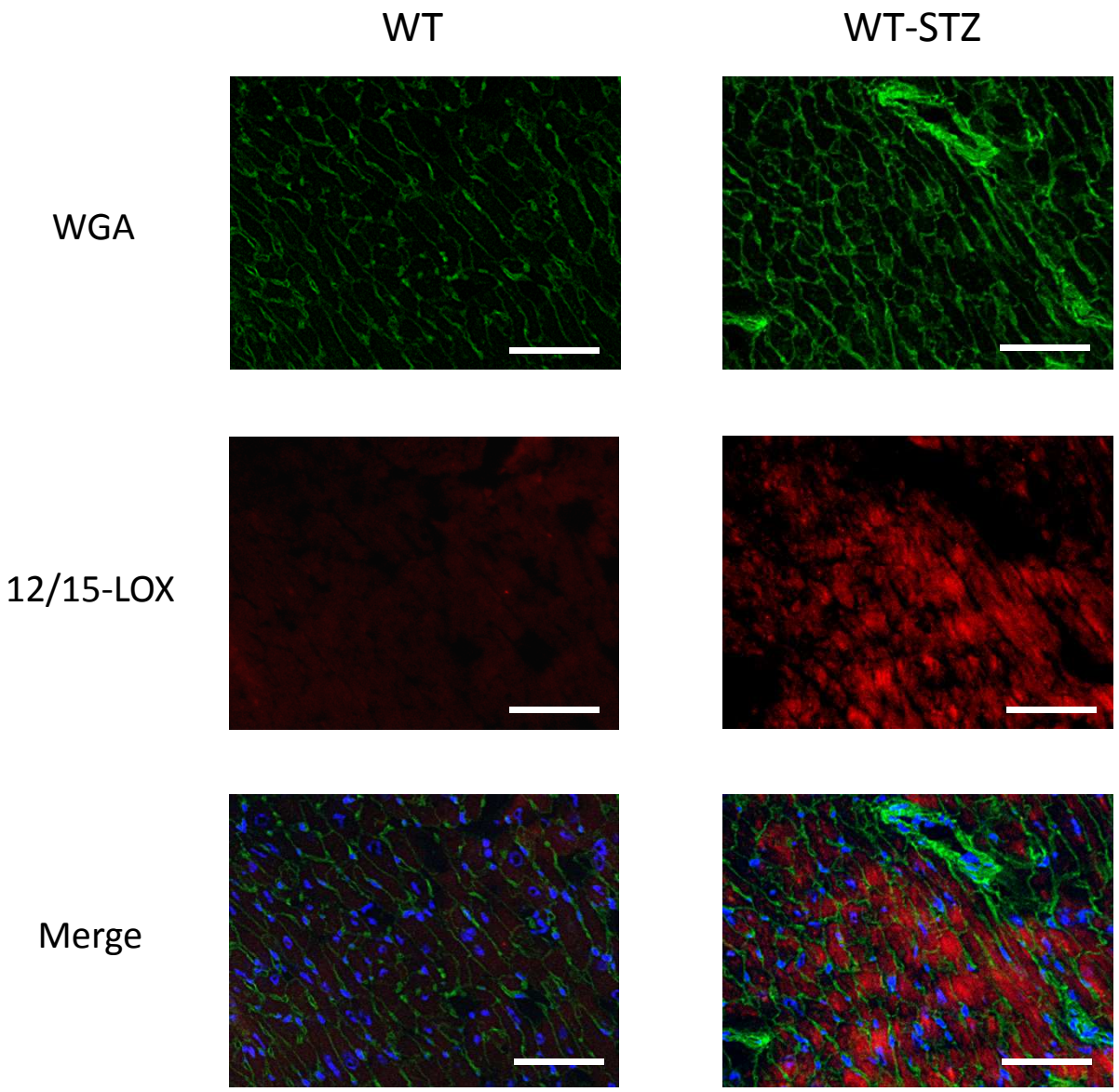

Figure 2A

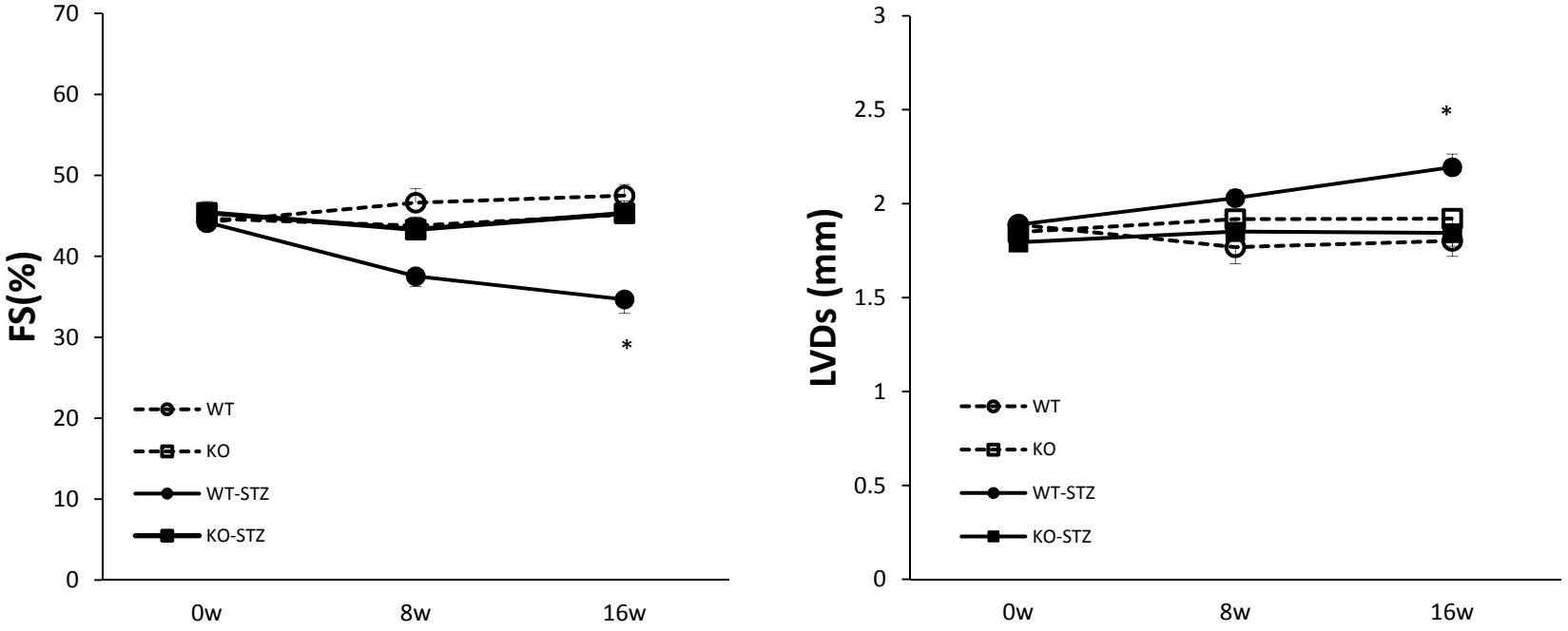

N=10-15, * : P<0.05, # : P<0.05

Figure 2B

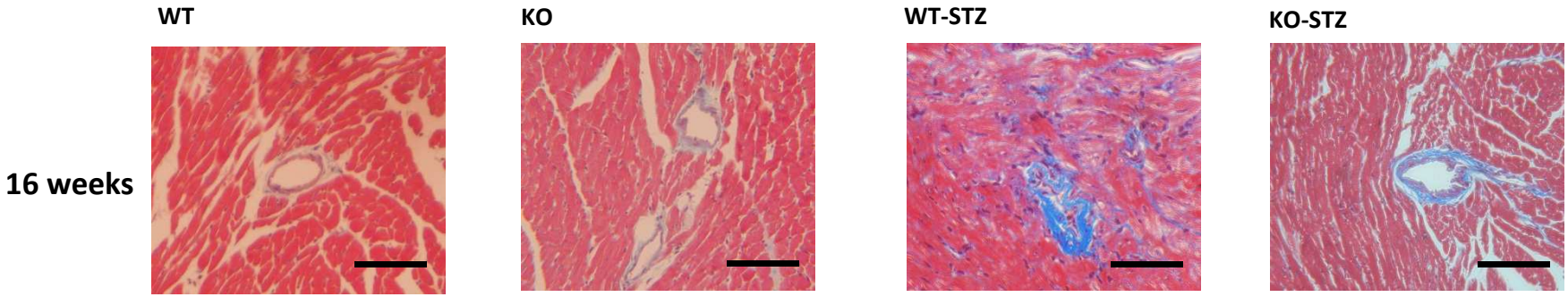

Masson stain Bar.60μm x200

Figure 2C

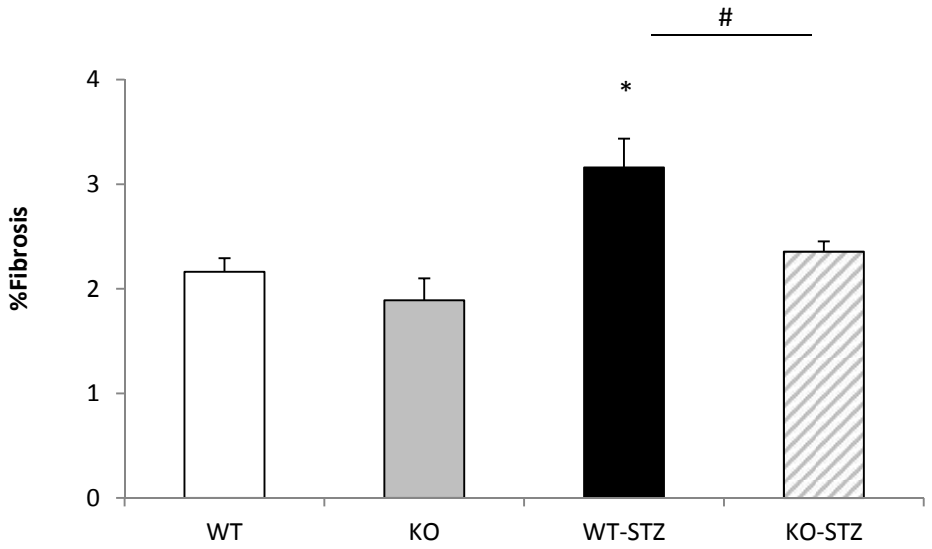

N=7-10, * : P<0.05, # : P<0.05

Figure 3A

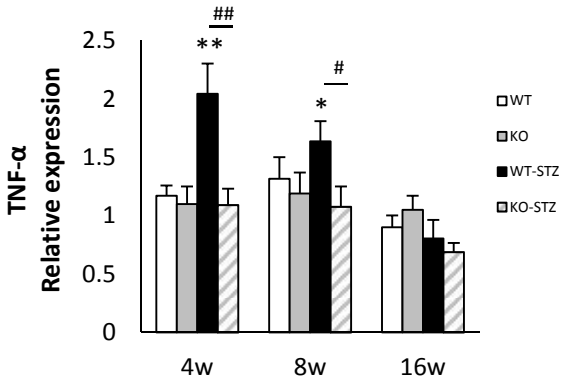

Figure 3B

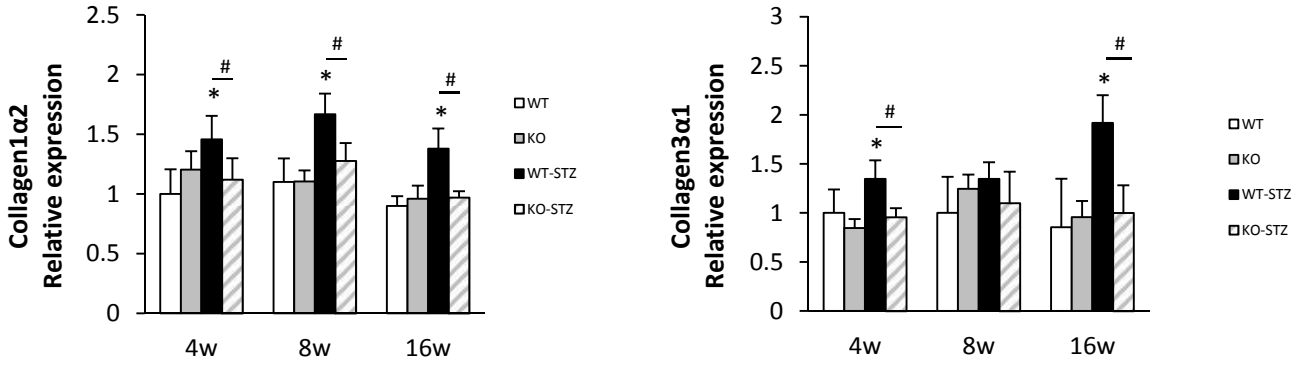

N=7-10, *P<0.05, **P<0.01 #P<0.05 ##P<0.01

Figure 3C

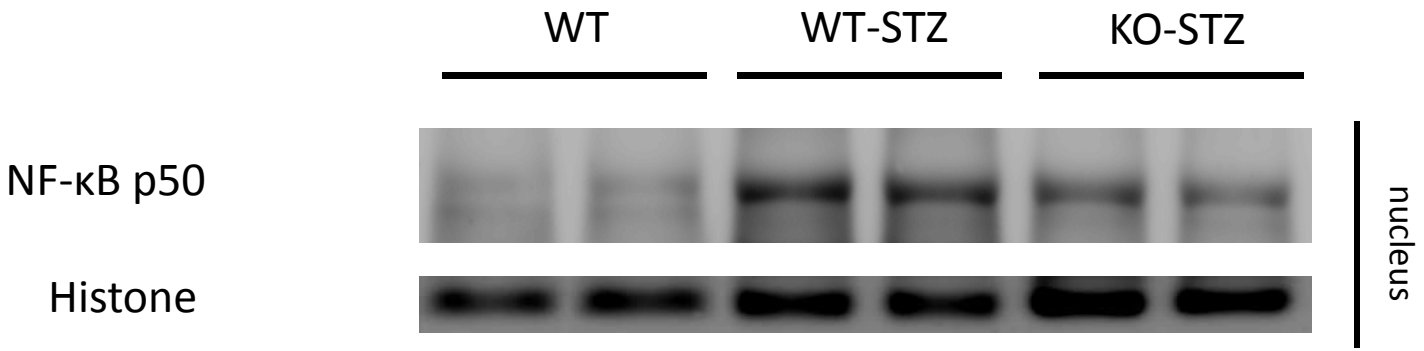

Figure 3D

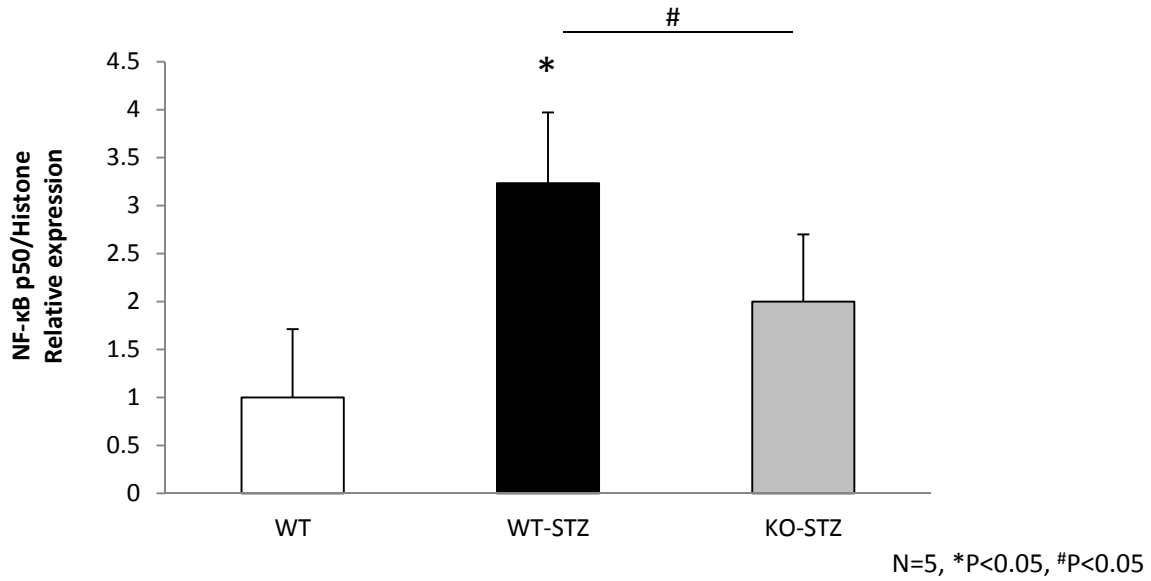

Figure 4A

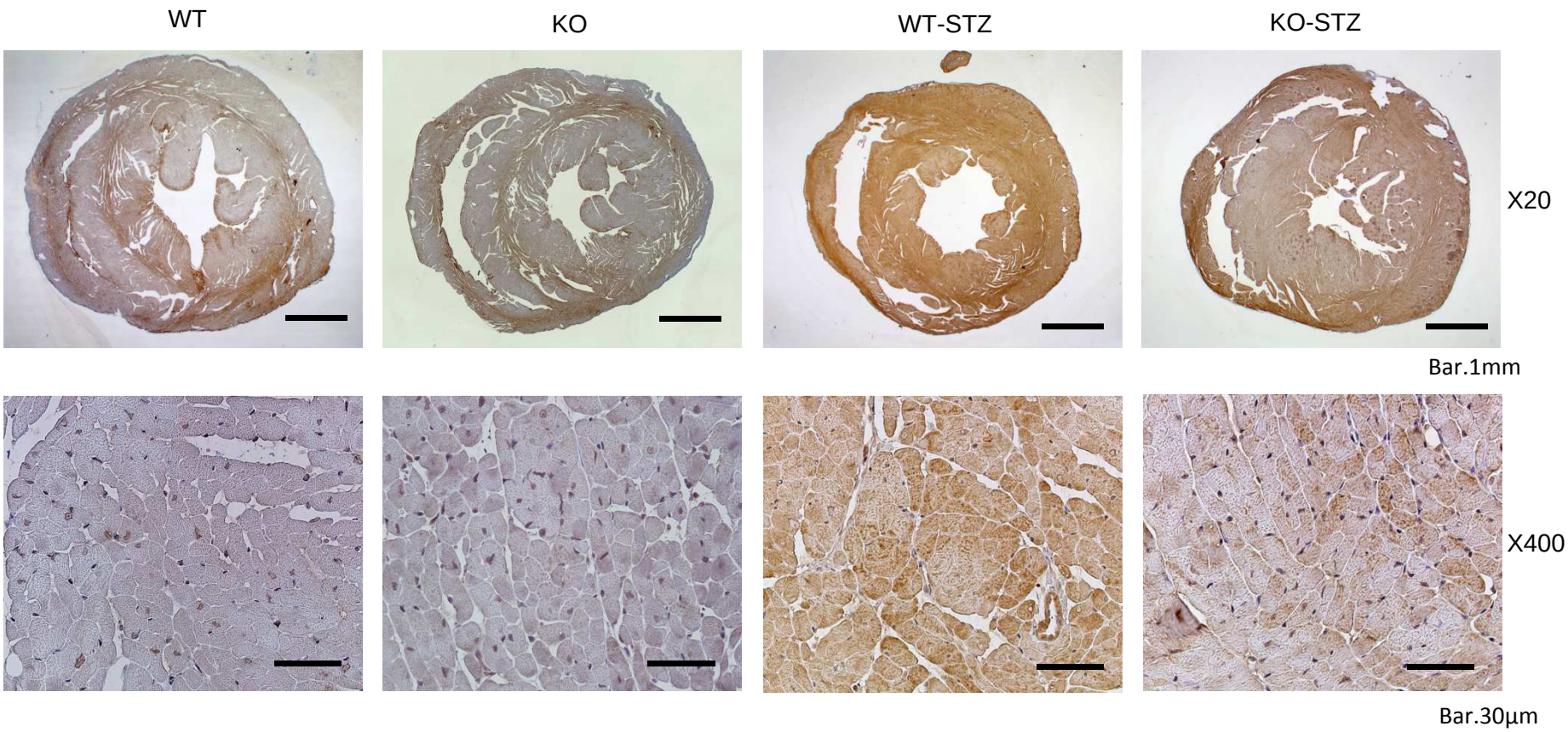

Figure 4B

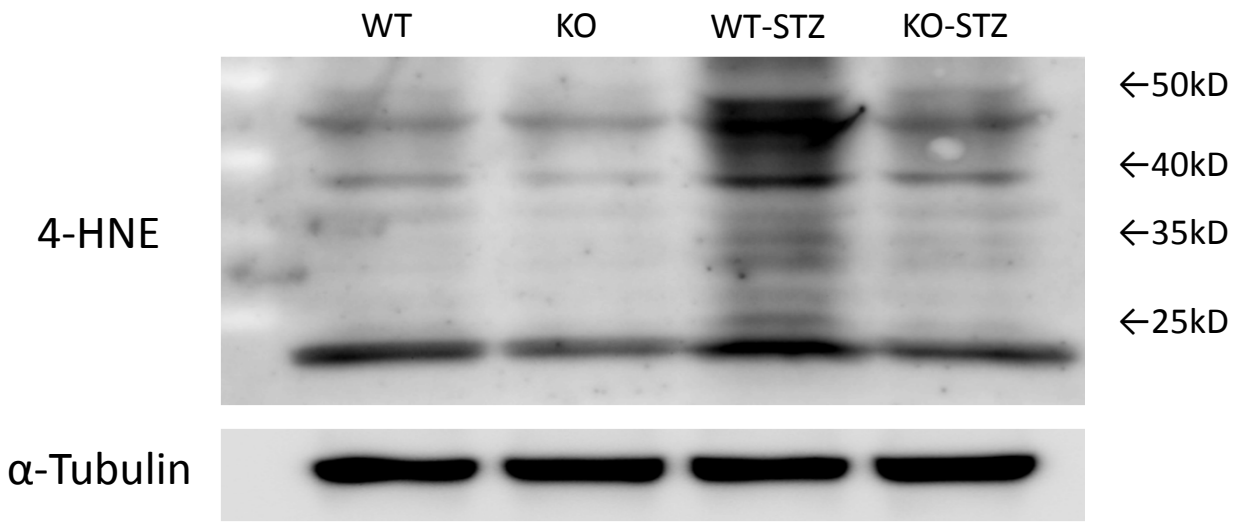

Figure 4C

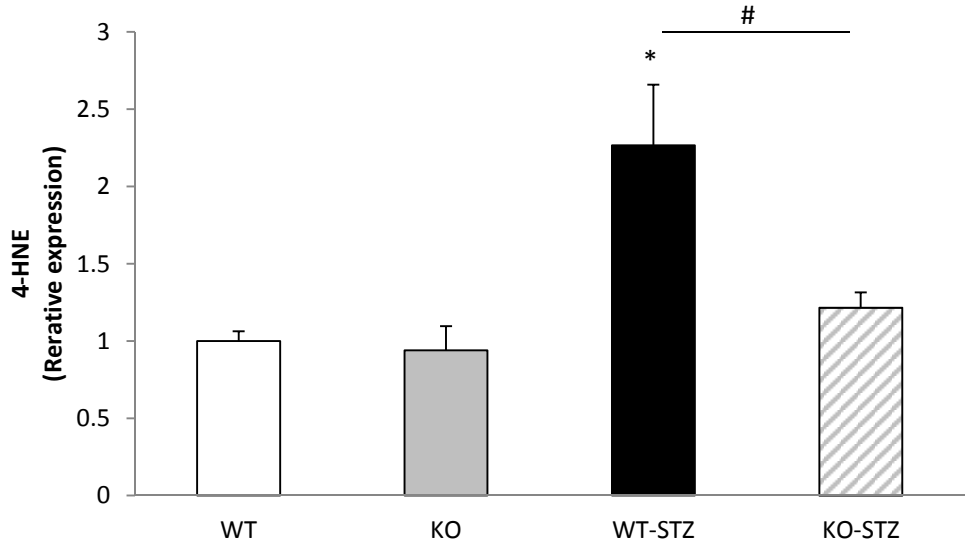

N=4, *P<0.05, #P<0.05

Figure 4D

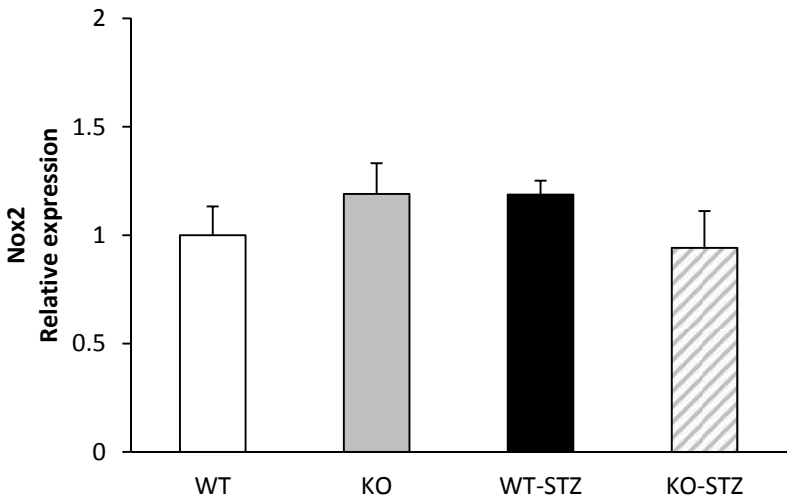
Nox2
Relative expression
2
1.5
1
0.5
0
WT
KO
WT-STZ
KO-STZ

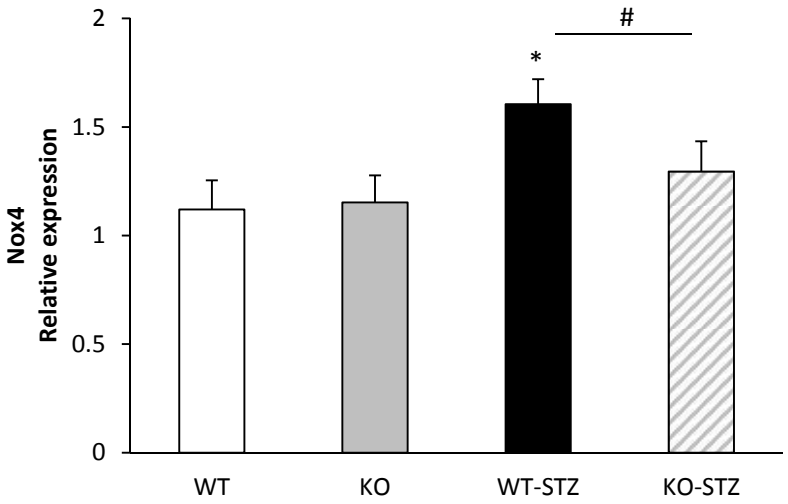
Nox4
Relative expression
2
1.5
1
0.5
0
*
#
WT
KO
WT-STZ
KO-STZ

Figure 4E

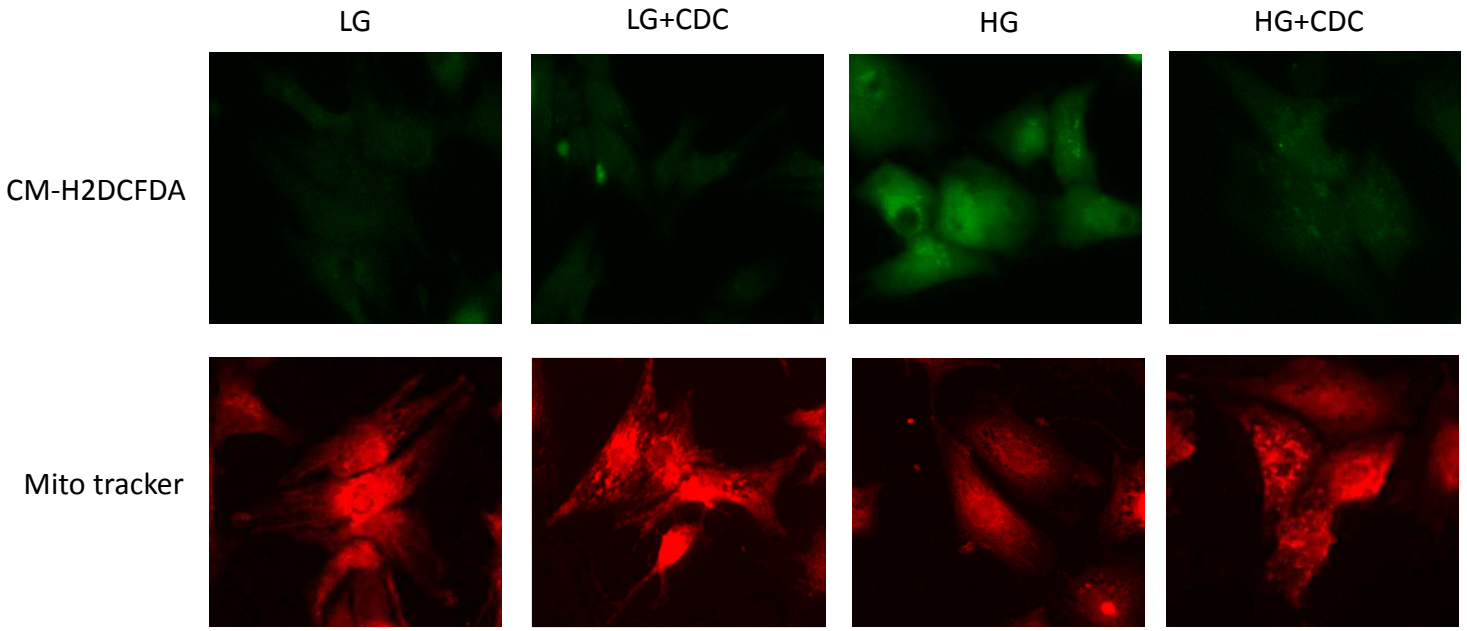

Figure 4F

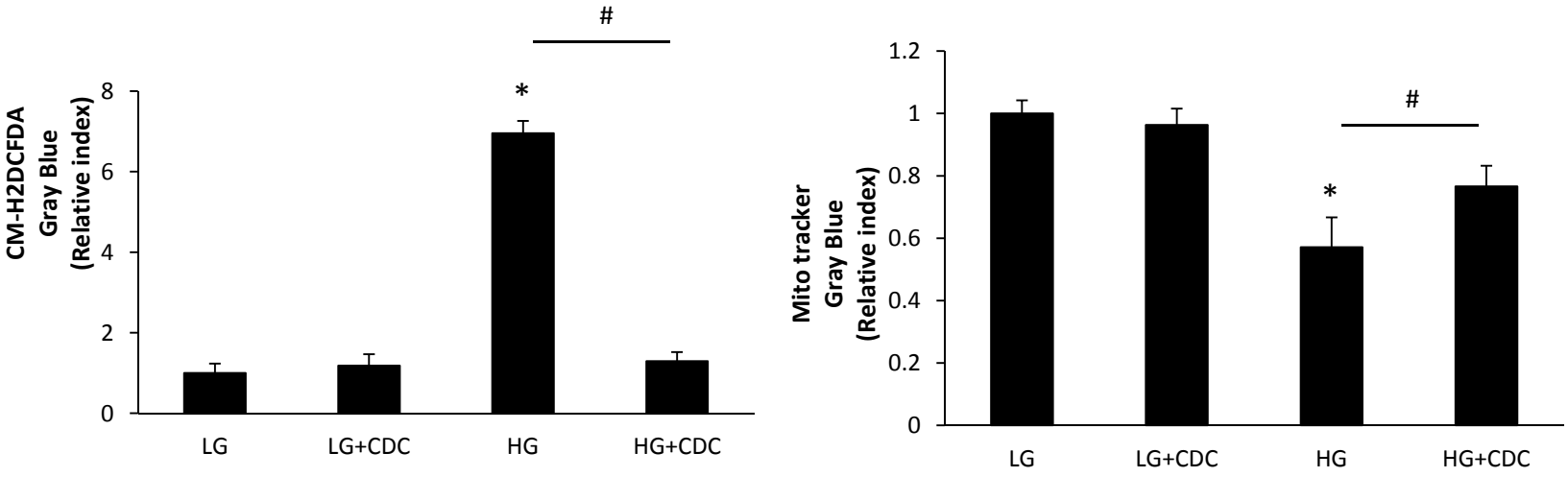

Figure 5A

16 weeks

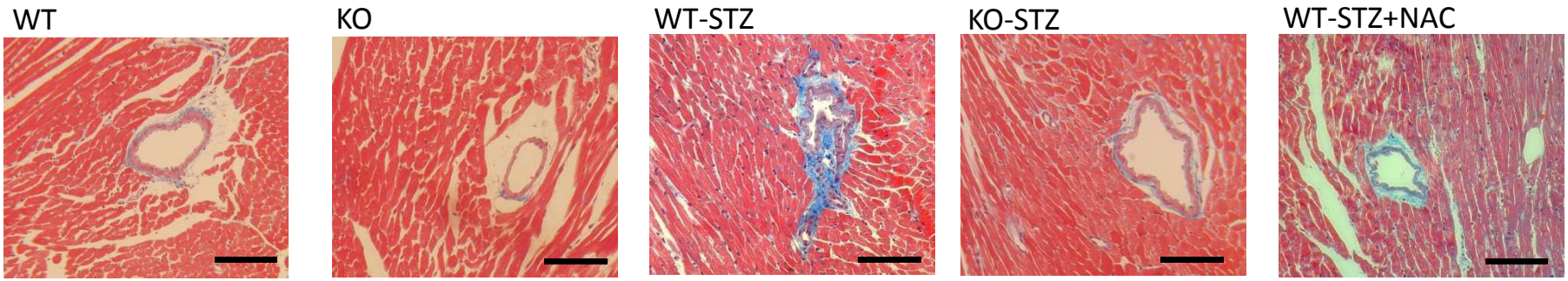

Masson stain Bar.60μm x200

Figure 5B

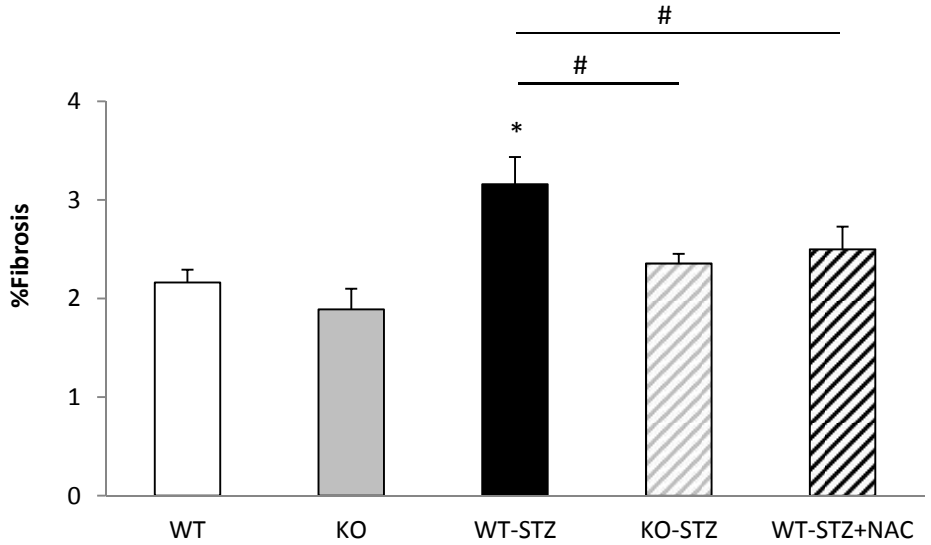

N=7-10, * : P<0.05, # : P<0.05

Figure 5C

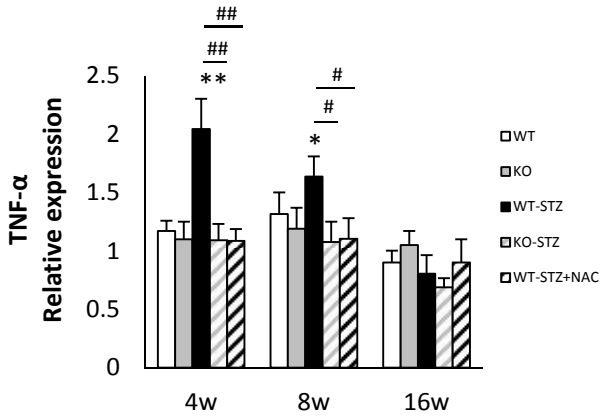

Figure 5D

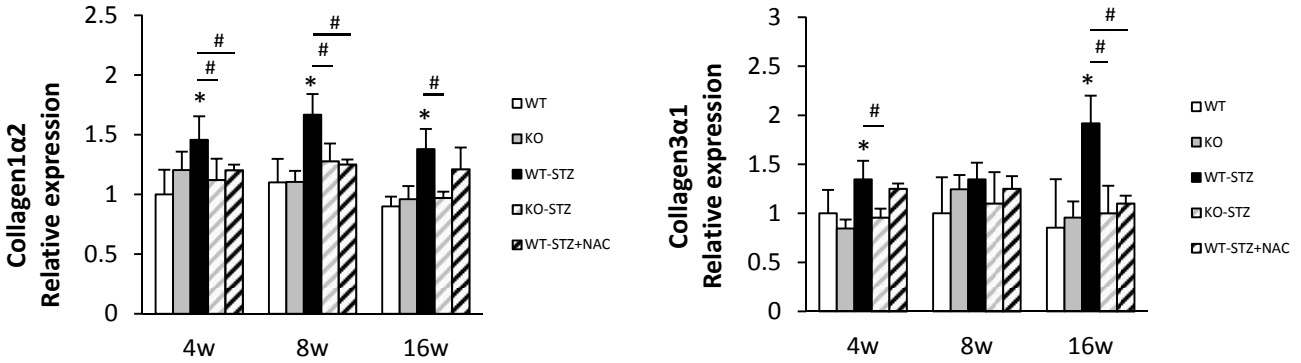

N=5-10, *P<0.05, **P<0.01 #P<0.05, ##P<0.01

Figure 6A

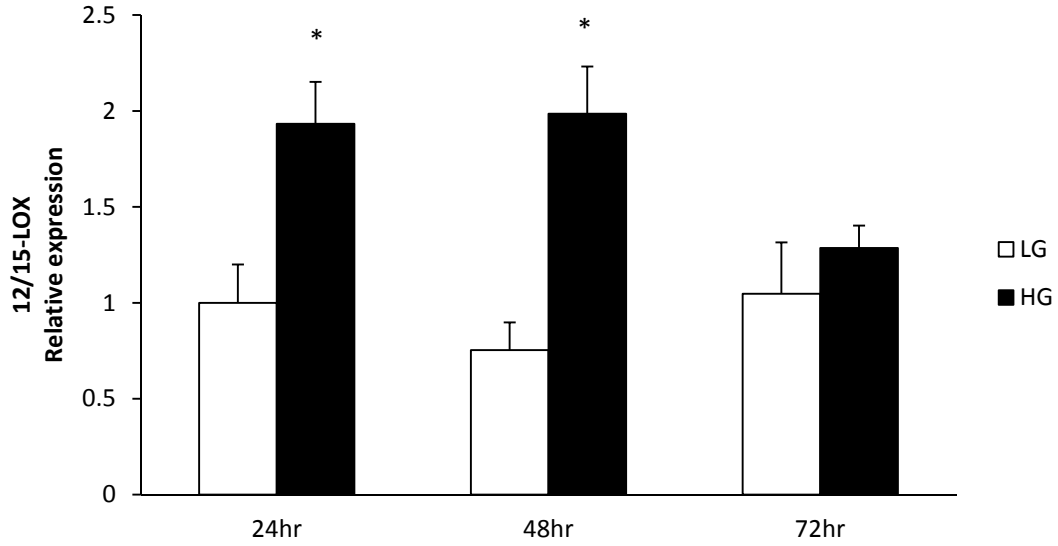

N=4-7, *P<0.05

Figure 6B

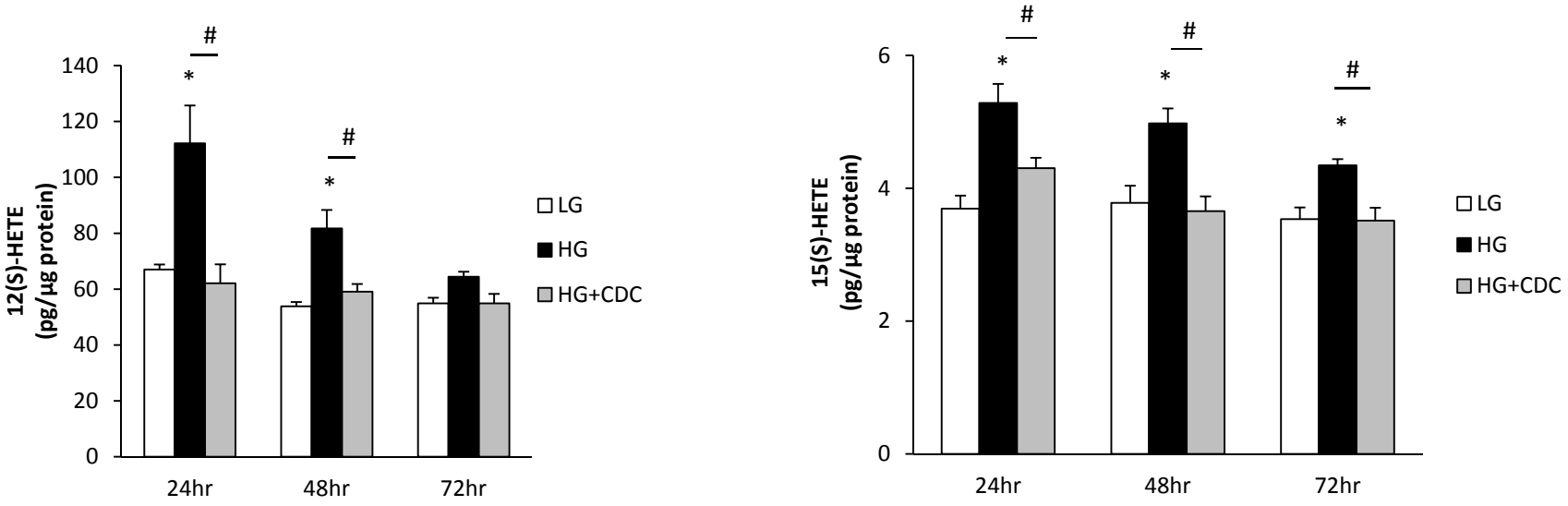

N=4-7, *P<0.05

Figure 6C

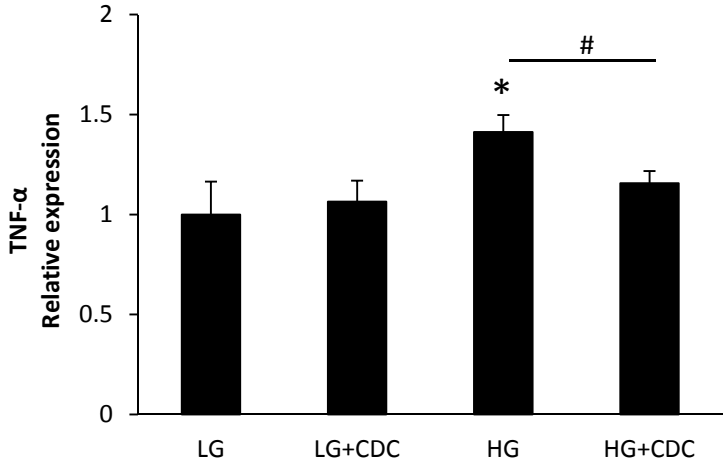

Figure 6D

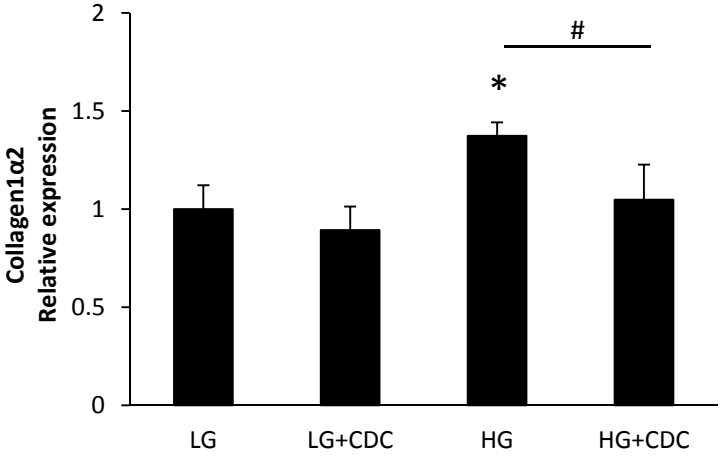

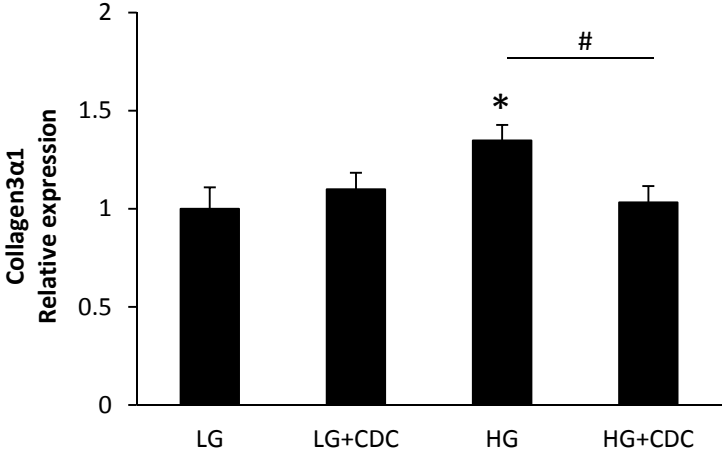

N=4-7, *P<0.05, #P<0.05

Figure 7A

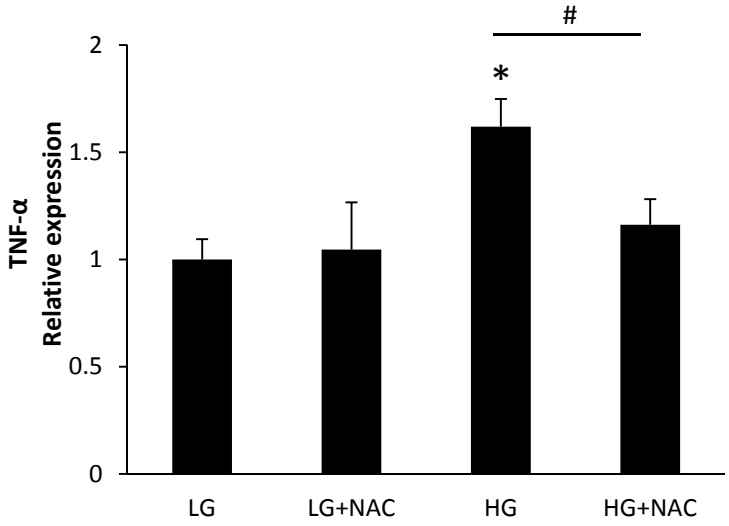

Figure 7B

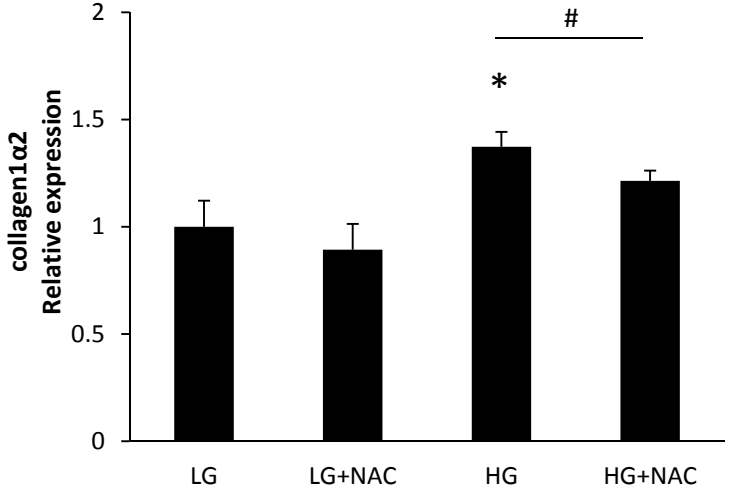

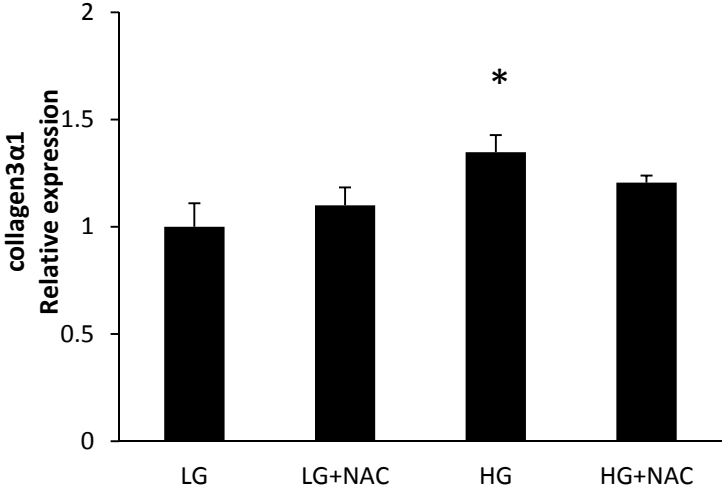

N=4-7, *P<0.05, #P<0.05

Figure 7C

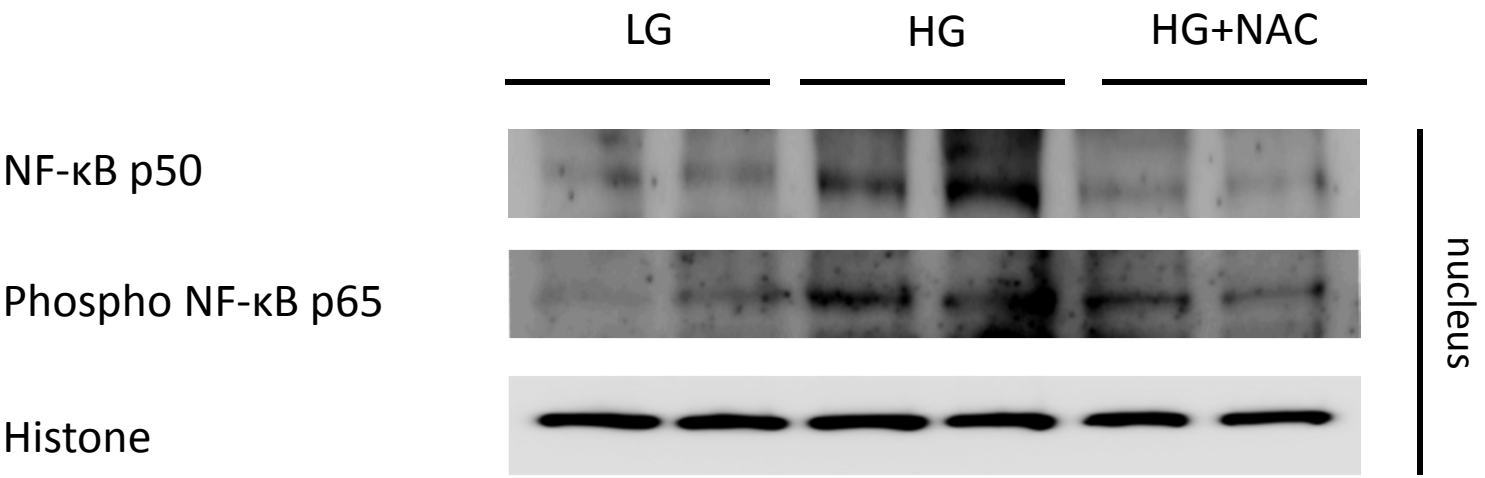

Figure 7D

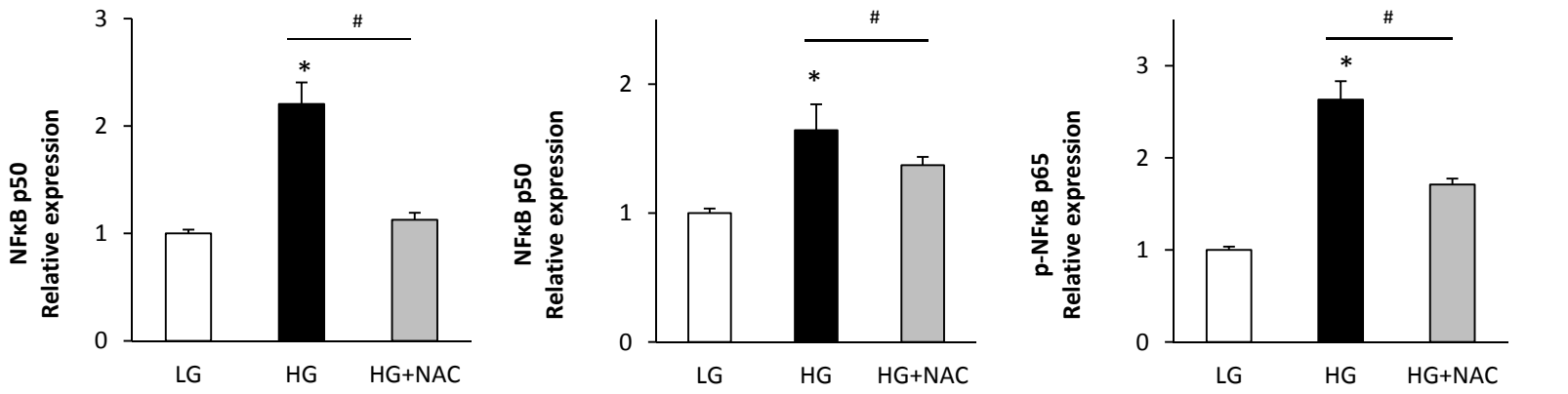

N=5, *P<0.05, #P<0.05

Supplementary figure1

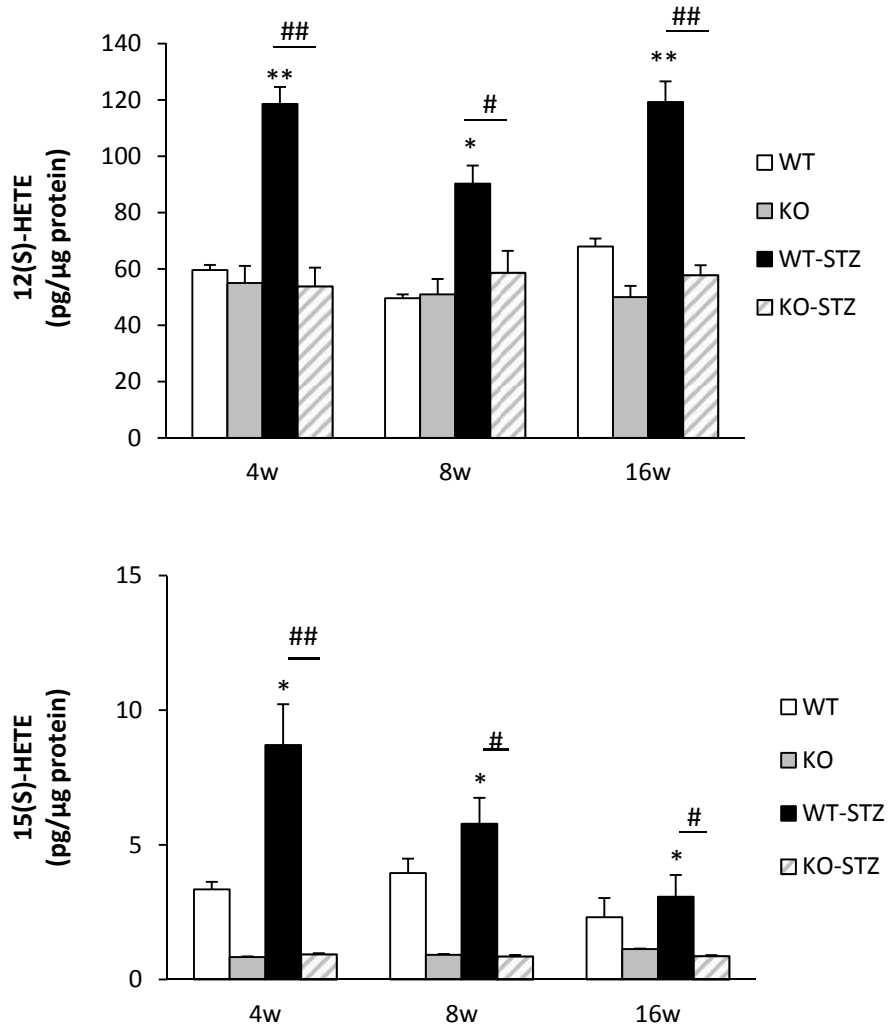

Supplementary figure 2

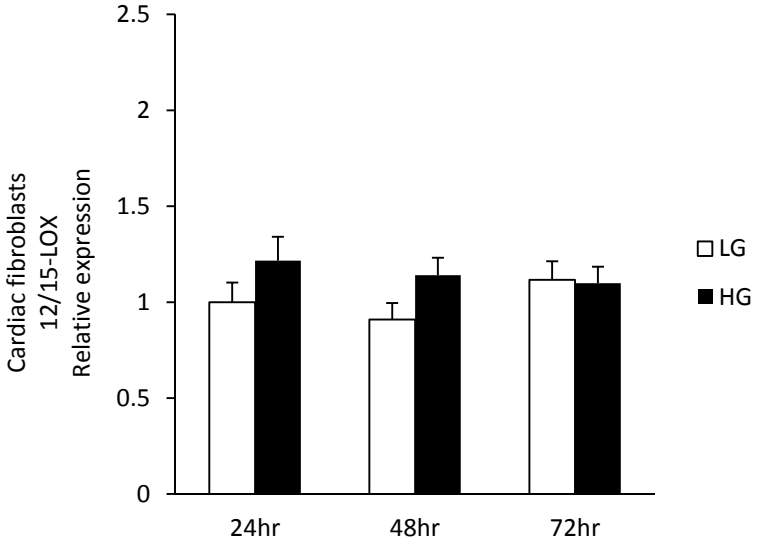

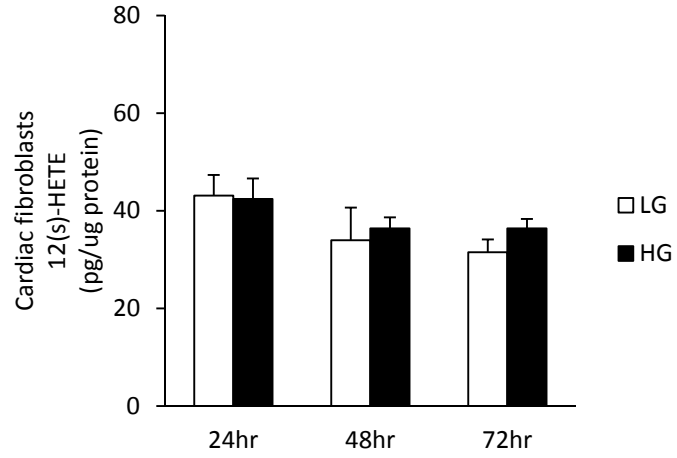

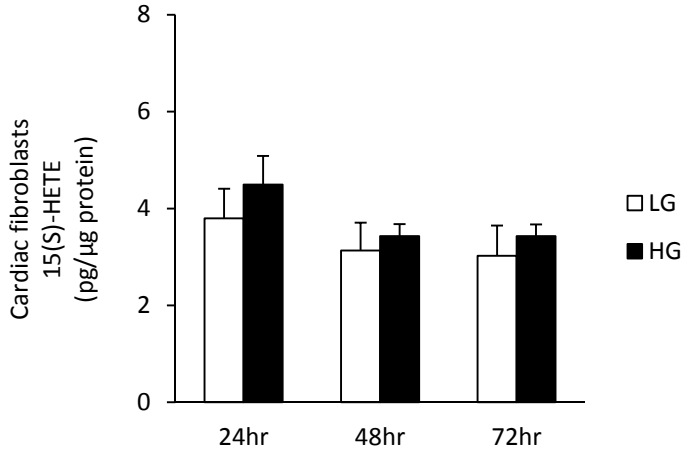

Supplementary figure 3A

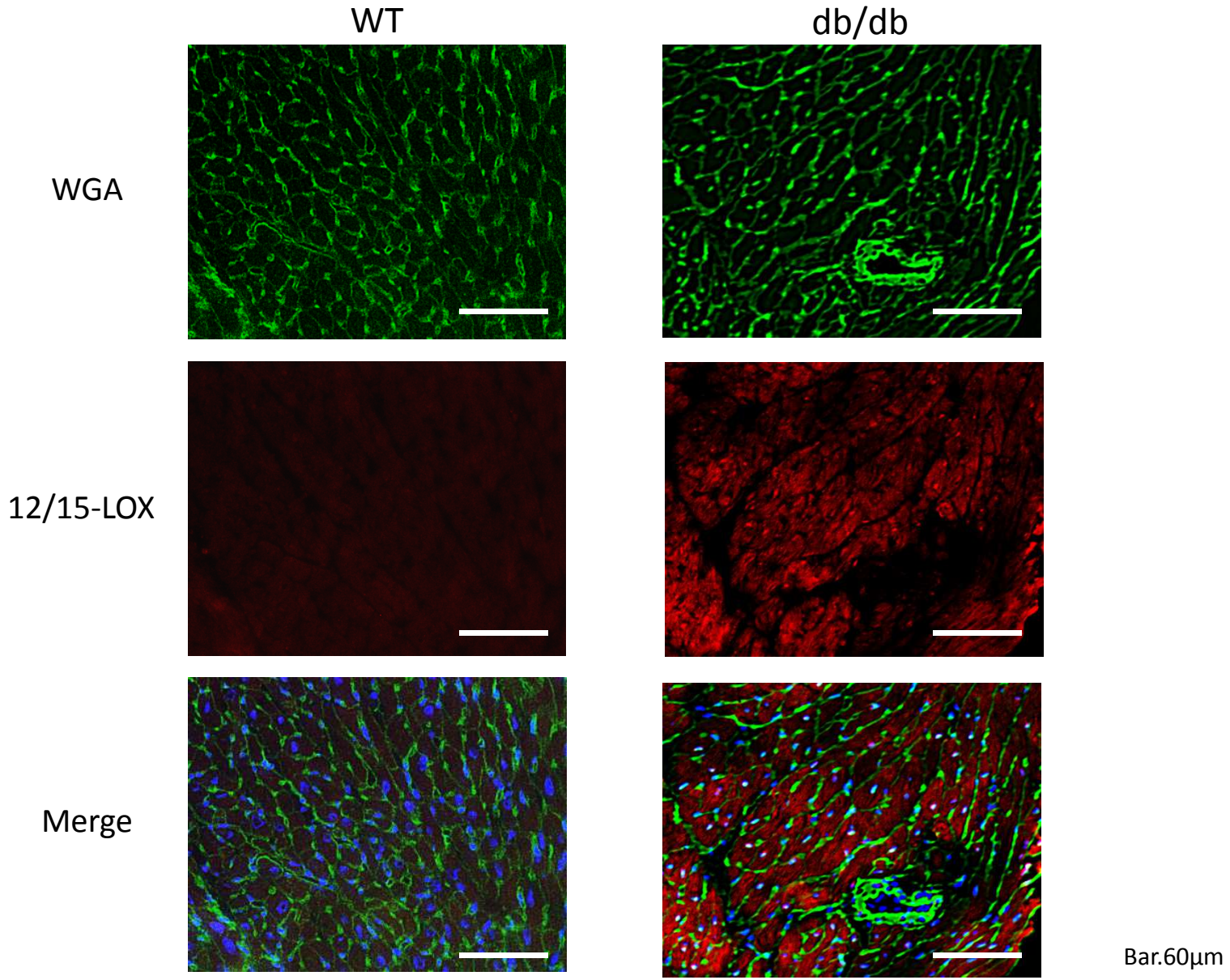

Supplementary figure 3B

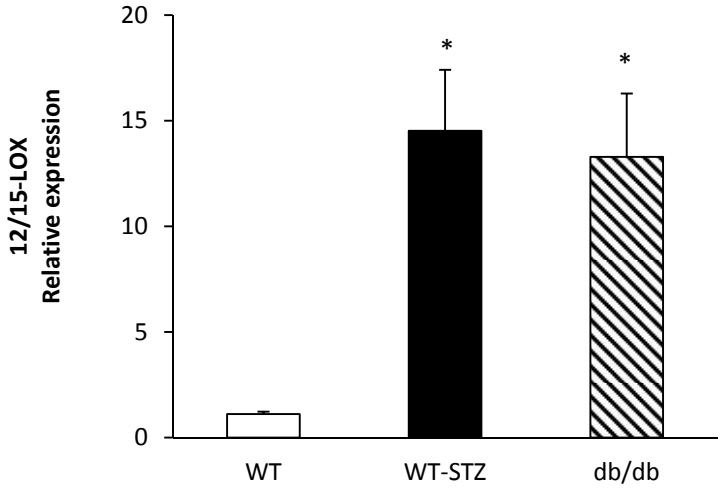

Supplementary figure 3C

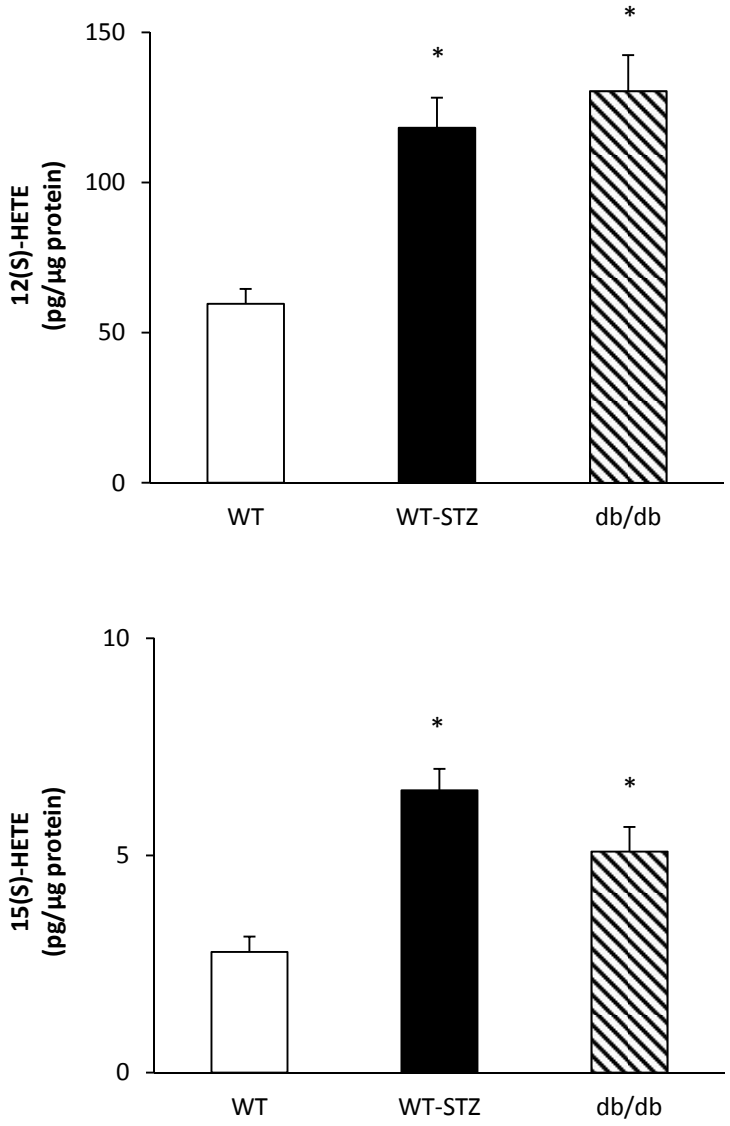

Supplementary figure 4

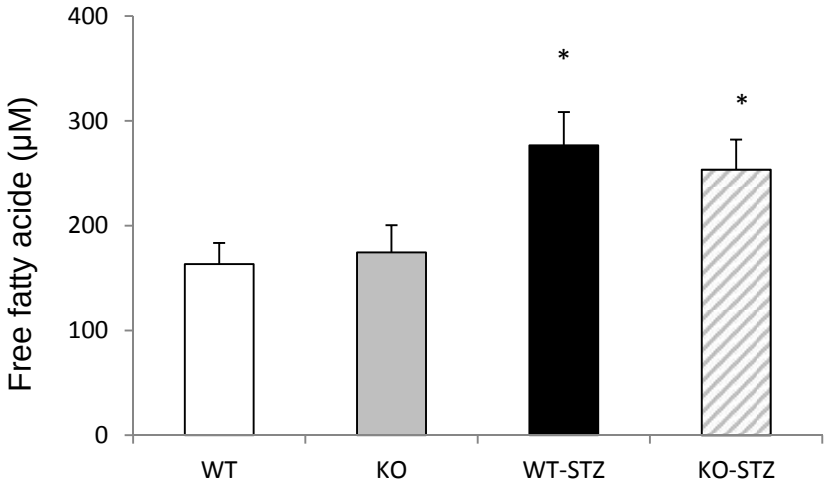

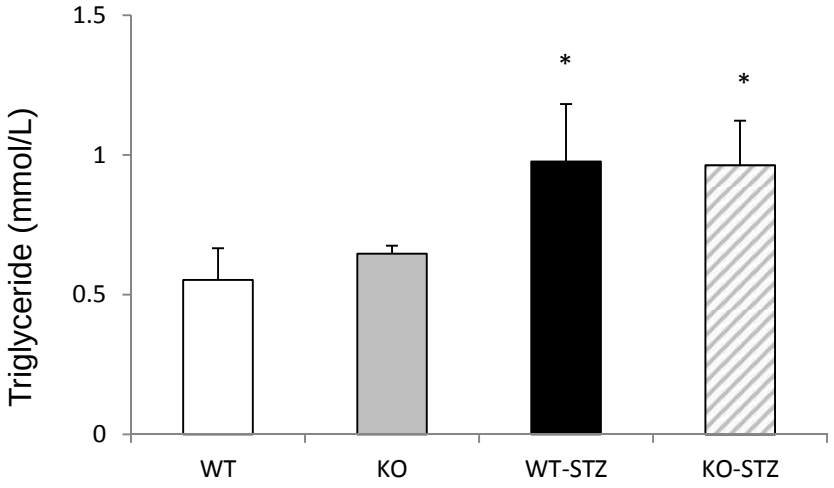

Supplementary figure 5

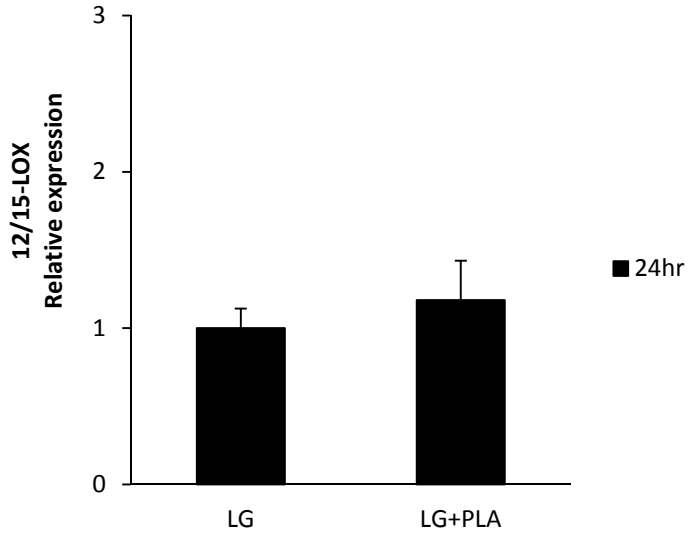

Palmitic acid (100uM)
N=4

Supplementary figure 6

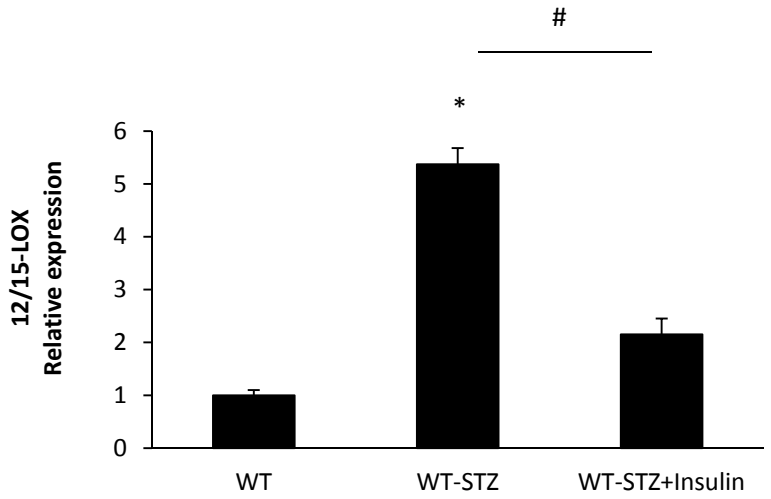

N=4-6, *P<0.05, #P<0.05

Supplementary figure 7

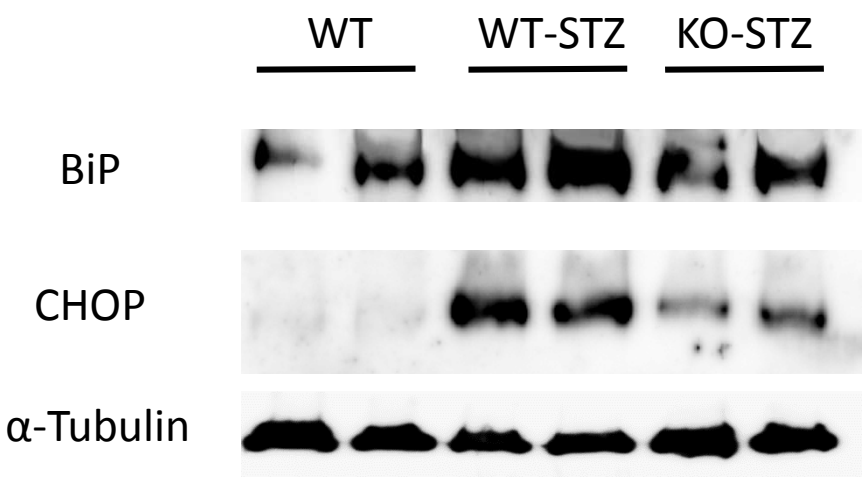

Supplementary figure 8